Diploma thesis

Autophagic markers in heart failure of different etiologies

submitted by

Amanjit Walter

in partial fulfillment of the requirements for the degree of

Doctor medicinae universae

(Dr. med. univ.)

at the

Medical University of Graz

executed at the

Division of Cardiology

under the supervision of

Univ.FA.Priv.-Doz. Dr.med. Dr.scient.med. Markus Wallner

Ass.-Prof. Senka Holzer, PhD

Graz, 23.11.2022

Statutory declaration

I hereby declare on my honor, that I have written this thesis independently and without external help, that I have not used any sources other than those indicated and that I have marked the passages taken verbatim or in content from the sources used as such.

Graz, 23.11.2022 Amanjit Walter m.p.

Acknoledgements

First, I want to thank both my supervisors, who made this thesis possible in the first place. A special thank goes to Ass-Prof in Senka Holzer, PhD for her advice on the results and her patience with my writing. And I thank Priv.-Doz. Dr.med. Dr.scient.med. Markus Wallner for his uncomplicated way of helping me out with organizational matters regarding this thesis.

My sincere thank also goes to Julia Voglhuber, MSc and Ingrid Matzer, MSc. Without their help and advice, I would not have been able to conduct my experiments.

My gratitude also reaches my boyfriend Thomas, who helped me especially in this matter with support and advice.

Thank you to my best friend Miriam, to whom I can always talk to and burden her with everything on my mind.

Last but not least my parents, who made it possible for me to study abroad and support me in no matter what.

Table of contents

List of abbreviation

Ambra1	activating molecule in beclin-1-regulated autophagy
Atg	autophagy related genes-protein
DCM	dilated cardiomyopathy
EF	(left ventricular) ejection fraction
Hsc70	heat shock cognate protein 70
HSD	high salt diet, 8% NaCl
KFERQ	pentapetide motif in many cytosolic proteins
Lamp2A	lysosomal-associated membrane protein 2A
LC3	microtubule-associated protein 1A/1B-light chain 3
LC3-I	soluble form of LC3 with C-terminal glycine for modification
LC3-II	syn. LC3-PE, LC3 linked to phosphatidylethanolamine
LSD	low salt diet, 0.3% NaCl
lyHsc70	lysosomal Hsc70
mTOR	mechanistic (mammalian) target of rapamycin
NCX1	sodium-calcium-exchanger 1
p62	ubiquitin-associated protein p62
PI3P III	class III phosphatidylinositol 3-kinase
Pink1	phosphatase and tensin homolog PTEN-induced kinase 1
ROS	reactive oxygen species
SERCA2a	sarco-/endoplasmatic reticulum Ca-ATPase 2a
TFEB	transcription factor EB
ULK1	Unc-51 like autophagy activating kinase
Vps	vacuolar protein sorting

List of figures

List of tables

Abstract (Deutsch)

***Einleitung**:* Autophagie ist ein wichtiger, physiologischer Mechanismus in der Homöostase eukaryotischer Zellen, um zelluläre Abfälle abzubauen und zu recyceln. Es gibt verschiedene Formen von Autophagie, welche verschiedene Arten von zellulärem Abfall verstoffwechseln können und abhängig sind von jeweiligen Regulationsmechanismen. Vor allem postmitotische Zellen sind auf Autophagie angewiesen, da sie sich nicht durch mitotische Zellteilung regenerieren können. Demnach sind auch Kardiomyozyten von einem intakten Autophagiemechanismus abhängig, um die normale Herzfunktion aufrechtzuerhalten. Neben dieser physiologischen Bedeutung ist Autophagie auch relevant in einigen pathophysiologischen Prozessen. Sowohl übermäßige Hoch- als auch Herunterregulierung der Aktivität ist zellschädlich. Diese Diplomarbeit wird sich mit Makroautophagie und Mitophagie befassen, durch Messung von Autophagiemarkern aus kardialem Gewebe von Menschen und Ratten, mit zugrunde liegenden unterschiedlichen kardialen Leiden.

***Methode**:* Zu diesem Zwecke wurden 7 Wochen alte männliche Dahl Salz-sensitive Ratten auf verschiedene Diäten gesetzt. Um kardiales Remodeling zu induzieren, wurde einer Subgruppe 8% NaCl Salz-reiche Diät verfüttert, während die Kontrollgruppe eine 0.3% NaCl Salz-arme Diät erhielt. *In-vivo* Phänotypisierung mit Blutdruckmessung wurde in zweiwöchigen Intervallen durchgeführt, die Salz-arme Gruppe und ein Teil der Salz-reichen Gruppe (Frühstadium des kardialen Remodelings) wurden nach 5 Wochen Diät geopfert, um linksventrikuläres Herzgewebe zu sammeln. Die übrig gebliebenen Ratten führten die Salz-reiche Diät fort (Spätstadium des kardialen Remodellings) und nach weiteren 5 Wochen wurde die Prozedur wiederholt. Zur Untersuchung von menschlichem Gewebe wurde von der Abteilung der Herzchirurgie der Medizinischen Universität Graz freundlicherweise Proben zur Verfügung gestellt. Es handelte sich um Gewebe aus dem linken Ventrikel von Herzen ohne Herzinsuffizienz, welche als Kontrolle dienten, und von Herzen mit diastolischer Dysfunktion und dilatativer Kardiomyopathie.

Die Zelllysate des linken Ventrikels vom Menschen und Nager wurden für Western Blot Analysen genutzt, um Autophagiemarker (p62, Atg5, LC3B, Parkin, Pink1) und den Autophagieregulatur mTOR zu untersuchen.

Ergebnisse: Im Rattemodell konnten wir zeigen, dass im Spätstadium des kardialen Remodelings ein signifikanter Anstieg von LC3B und Parkin stattfand. Änderungen in anderen Autophagiemarkern erreichten keine Signifikanz. In menschlichen Proben mit diastolischer Dysfunktion konnten keine signifikanten Ergebnisse erzielt werden. Diese wurden nur in menschlichen Proben von dilatativer Kardiomyopathie erzielt, mit einem signifikanten Anstieg von mTOR und p-mTOR. ***Diskussion***: Bei den hypertensiven Dahl Salz-sensitiven Ratten haben wir eine verminderte Autophagie-Aktivität erwartet. Unsere Ergebnisse haben dies nur teilweise bestätigen können. Um die Ergebnisse mit Widerspruch oder fehlender Änderungstendenz erklären zu können, müssen weitere Untersuchungsmethoden angewandt werden. Dies trifft auch auf die Ergebnisse aus den menschlichen Proben zu. Außerdem könnte eine Vergrößerung des Probenumfanges helfen, die zu erwarteten Ergebnisse zu zeigen, da einige Resultate bereits Tendenzen zeigten, dabei allerdings noch keine Signifikanz erreichten.

Abstract (Englisch)

***Introduction**:* In eukaryotic cell homeostasis, autophagy is an important physiological mechanism to process cellular debris in order to disassemble and recycle them. There are different autophagy mechanisms digesting different cargo, and they are dependent on various regulatory mechanism. Especially postmitotic cells are dependent on autophagy, for they are unable to regenerate by mitosis. Like in cardiomyocytes, intact autophagy machinery is crucial for normal cardiac function. Beside that physiological importance, autophagy is also relevant in pathophysiological context. Both excessively upregulated or downregulated autophagic activity is harmful. In this thesis, macroautophagy and mitophagy will be investigated for alteration of autophagy markers in human and rat hearts with different etiologies of heart failure.

***Method**:* For this purpose, 7 weeks old male Dahl salt-sensitive rats were set on different diets. To induce cardiac remodelling, a subgroup was fed an 8% NaCl high-salt diet (HSD) and for control, a subgroup was fed a 0.3% low-salt diet (LSD). *In vivo* phenotyping with blood pressure measurements was performed at two-weeks intervals, and the LSD group and a portion of the HSD group (early stage of cardiac remodelling) were sacrificed after 5 weeks of diet to collect left ventricular heart tissue. The remaining rats on HSD further continued their diet for 5 weeks (late stage of cardiac remodelling) and the procedure was repeated. For investigation of human samples, the clinical department for cardiosurgery of the Medical University of Graz provided left ventricular heart tissue selected from non-failing hearts to serve as control, and to compare from hearts with diastolic dysfunction and dilated cardiomyopathy (DCM).

For whole tissue cell homogenates of human and rat left ventricular myocardium, immunoblotting was performed to investigate markers of heart failure (NCX1, SERCA2a), autophagy-related proteins (p62, Atg5, LC3B, Parkin, Pink1) and the autophagy-regulator mTOR.

***Results**:* In the rat model, we could show that in the late stage of cardiac remodelling, there was a significant increase in LC3B and Parkin. Changes in the other autophagy-related proteins failed to reach significance. In the human samples of diastolic dysfunction, no significant findings were made. Those were only achieved in patients with DCM, there was a significant increase in both mTOR and

p-mTOR levels.

***Discussion**:* For hypertensive Dahl salt-sensitive rats, we expected downregulation of autophagy with regard to other data. Our results confirmed that only in partial. To clarify the ambiguous and unchanged results, further investigations and methods are necessary. This also applies for the data obtained in human samples. Also, an expansion of sample size could help to show the anticipated results, since some results already showed trends but without extend for significance.

.

1 Introduction

1.1 Autophaghy

The term autophagy, derived from the Greek term ‘autóphagos‘, can be translated with self-devouring and describes, along general lines, the process of degradation and removing unnecessary or dysfunctional components of the cell [1]. There are mainly three types of autophagy characterized in literature: macroautophagy, microautophagy and chaperon-mediated autophagy. It should be noted, that when the term autophagy is used, it commonly refers to macroautophagy. They all have in common, that there is a cellular component (from small cytoplasm portions to a whole organelle), the socalled ‘cargo‘, which is being digested by lysosomes in the process. To achieve this, depending on the autophagy mechanism, different autophagic structures are necessary [2].

1.1.1 Types of autophagy

1.1.1.1 Macroautophagy

In macroautphagy, a small portion of membrane is required to encircle a portion of cytoplasm or subcellular organelles. This membrane portion is called isolation membrane (syn. phagophore) and can originate from different cell compartments. As soon as the isolation membrane has fully engulfed and isolated its cargo from the cytoplasm, the bilayerd complex is called autophagosome. Macroautophagy represents the main type of autophagy and is highly inducible by stimuli and metabolic conditions described later. The formation of the isolation membrane needs preformed membranous structures. The endoplasmatic reticulum (ER) is broadly reported to be the location where isolation membranes are formed. But it is also suggested, that they can originate from Golgi apparatus, mitochondria and even plasma membrane [2, 3]. The following description refers to the ER as the formation site. The formation is a process involving complex formation units, e.g. **Atg proteins**. The ULK1-complex (composed of ULK1, Atg13, Atg101 and FIP200 (focal adhesion kinase family interacting protein of 200 kD)) starts the induction of formation and activates a second complex, composed of Beclin1 which has to be

recruited from the ER membrane, Atg14, Ambra1, Vps15 and 34 [2, 4]. Vps34 is also known as PI3K class III and must not be confused with PI3K in Akt/mTOR pathway [5]. This second complex initiates PI3P (phosphatidylinositol 3-phosphate) synthesis at the membrane of the ER, which mediates translocation of autophagy-related proteins, such as WIPI's (WD-repeat protein interacting with phosphoinositides) and DFCP1 (double FYVE-containing protein 1) to the formation site (promotion of elongation and maturation of the omegasome). The omegasome is the portion of the ER membrane, which begins to shape into the later isolation membrane, but is still connected to the ER (shaped like an ‚omega' Ω, see Figure 1-1). Elongation and closure of the omegasome is also promoted by the Atg12-5-16L conjugate, as well as the integration of **LC3** protein into the newly formed omegasome/early isolation membrane, see Figure 1-2 and 1-3. Somehow, the matured omegasome detaches from the ER and an isolation membrane is released, Figure 1-1 [2].

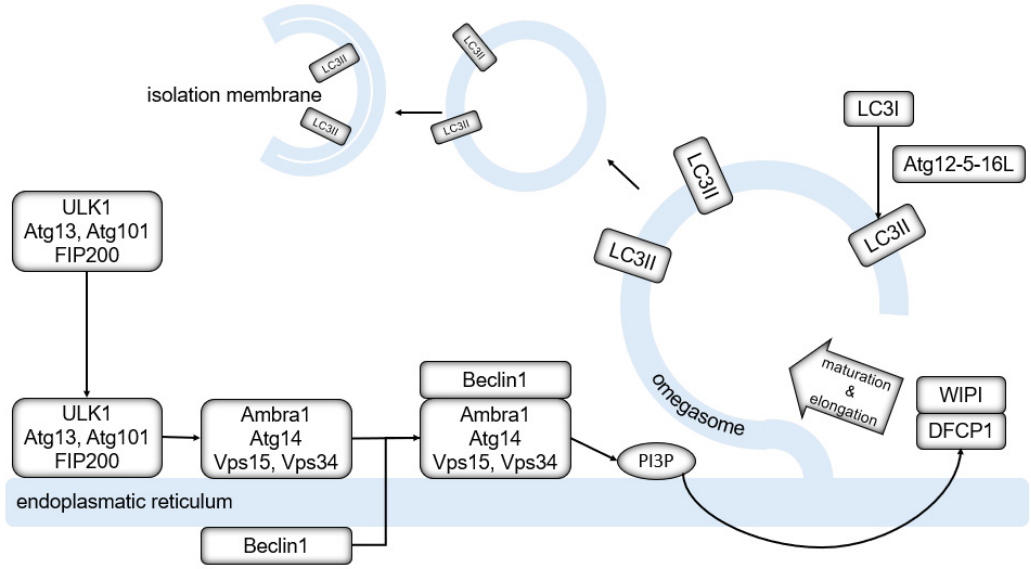

Figure 1-1: **Formation mechanism of the isolation membrane**: See description in text. Inspired by Mizushima, N. and Komatsu, M. [2].

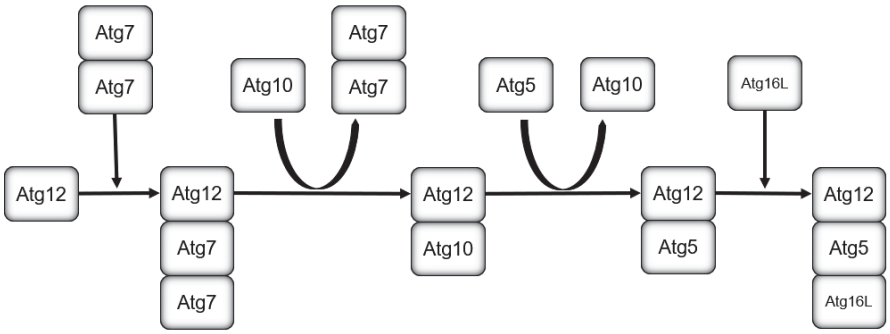

Figure 1-2: Atg12-5-16L formation: Composition of Atg12-5-16L conjugate requires of course Atg5, 12 and 16L, but also additionally Atg7 and 10 as ‚constructors'. Atg7 (operating as homodimer) activates Atg12 and bonds reversible with it, thereby transferring Atg12 to Atg10, now forming a reversible bond between both, and Atg7 homodimer dissociates. Atg10 now mediates an irreversible bond between Atg 12 and 5, Atg 10 itself dissociates. The Atg5-Atg12 conjugate attracts and binds Atg16L, forming a threepart Atg5-Atg12-Atg16L conjugate. Four of those threepart conjugates associate to a tetrameric complex. Inspired by Randall-Demllo, S., Chieppa, M. and Eri, R. [6]

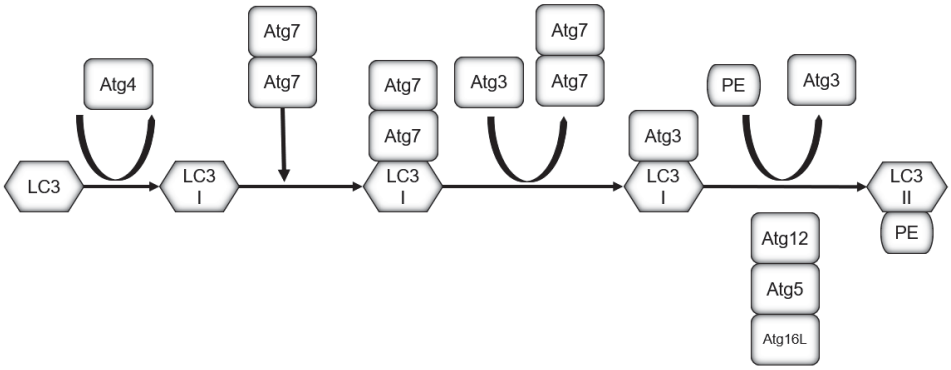

Figure 1-3: LC3-II formation and integration: First, Atg4 cleaves LC3 to prepare it for modification, now called LC3-I. Again, an Atg7 homodimer is needed, it binds reversible to LC3-I to recruit and transfer it to Atg3 and again, Atg7 homodimer dissociates. Atg3 mediates the conjugation of LC3-I to phosphatidylethanolamine in the ER membrane, Atg3 itself dissociates, forming LC3-II (syn. LC3-PE). This last step is supported and enhanced by Atg12-5-16L conjugate. Inspired by Randall-Demllo, S., Chieppa, M. and Eri, R. [6].

A main mechanism for cargo uptake in macroautophagy is mediated by the protein **p62**. On the one hand, there is the newly formed isolation membrane ready to operate and on the other hand, there is cargo waiting to be picked up. p62 is broadly expressed in any cell type and contains a region for LC3-II interaction. It further contains an ubiquitin-associated domain (UBA) for binding ubiquitinated cargo, so it appears as an adaptor/interface between cargo and isolation membrane and is

degraded during the process, Figure 1-4. The lower the autophagic activity, the lesser p62 is consumed. This may lead to accumulation of p62 within the cell (e.g. in neurodegenerative disease, p62 containing inclusion bodies were found). Beside p62, there are other adaptor proteins, e.g. NDP52 and optineurin to name a few. Their role is described in labelling intracellular invaded microbes for autophagy as part of immune defense [2, 7]. To degrade the included cargo, fusion with lysosomes is necessary to provide the proper set of enzymes. After fusion, the still bilayerd complex is called autophagolysosome [2]. The unilayerd lysosomal membrane and outer autophagosomal membrane form the outer autophagolysosomal membrane and the inner autophagosomal membrane remains as inner autophagolysosomal membrane and is decomposed with the content, Figure 1-4A and B [8].

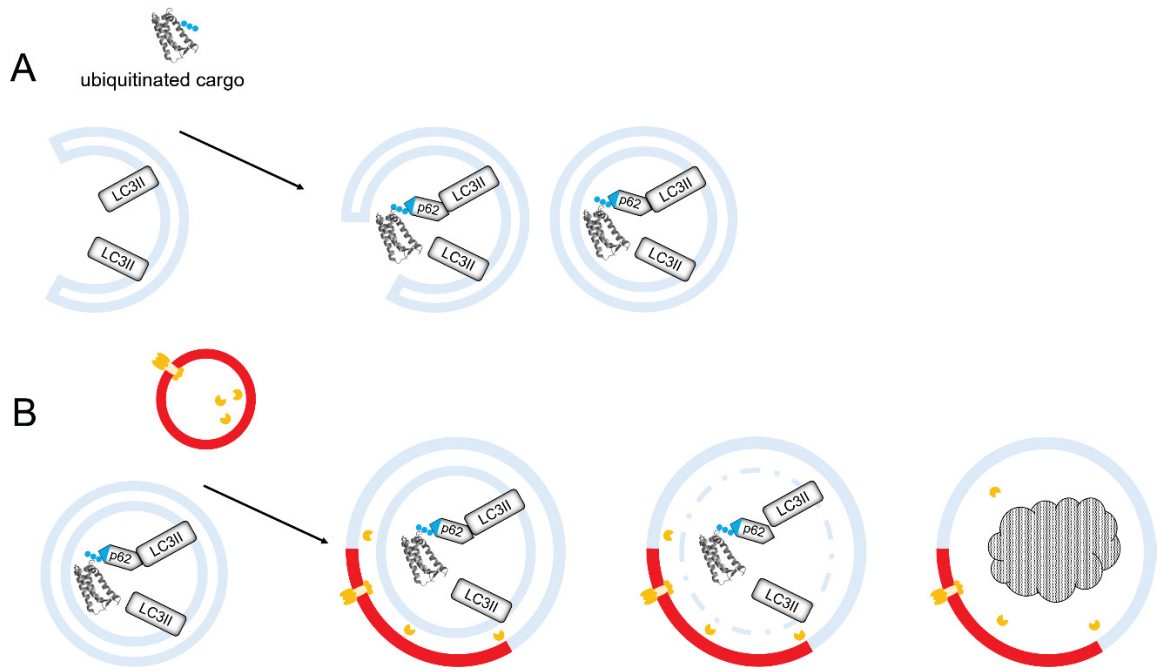

Figure 1-4: Cargo uptake and lysosomal fusion in macroautophagy: [A] Newly formed isolation membrane and binding of ubiquitinated cargo to LC3-II in isolation membrane, with p62 serving as adaptor between ubiquitin and LC3-II. Engulfment of bound cargo and closure to form an autophagosome. [B] Fusion of autophagosome with lysosome to form an autophagolysosome. After fusion, the inner layer of the autophagolysosome dissolves and the cargo is digested by lysosomal enzymes.

The regulation of macroautophagy is complex and there are numerous molecular participants that ensure proper maintenance of cellular components‘ clearance. One of the most important and well-studied autophagic regulator is **mTOR**, a kinase present in two forms of complexes with other proteins, mTORC1 and mTORC2. In this context, mTOR mainly shows as a major antagonist of autophagy and can maintain adverse cardiac remodelling and effects [9, 10]. Indeed, molecular and cellular components cannot be labeled as simply favorable or harmful, and there are conditions when mTOR activation benefits the cell. Here, however, we focus on mTOR function in hampering autophagy via different signaling pathways. For example, in aged hearts that show functional deterioration, higher mTOR activity can be observed. This is in line with the decreased levels of autophagy promoting factors in aged hearts, showing that with age the intracellular conditions shift to less autophagy activation [9]. mTORC1 inhibitorily posphorylates ULK1 and AMBRA1, Atg14L and Vps34, so the formation of autophagosomes arrests in an early state. Further, it represses the transcriptional activity of TFEB [11]. TFEB regulates the transcription of lysosomal and autophagosomal genes, including Atg genes. Activation of TFEB allows it to translocate to the nucleus to initiate gene transcription [12]. Among other important autophagy regulator factors, TFEB is downregulated in aged myocardium [13].

Two kinases, PI3K and Akt (serine/threonine-protein kinase akt), are involved in many intracellular signaling cascades, and one of their targets is the activation of mTOR. Other regulatory mechanism arise from mTOR representing an energy sensing kinase, therefore caloric restriction is shown to repress mTOR activity. AMPK (5-AMP-activated kinase) and GSK-3β (glycogen synthase kinase-3 beta) are kinases promoting autophagy, whose activity is also regulated by the energy status of the cell [9]. Their activation is promoted by low ATP levels and high AMP levels [12]. Furthermore, damage-associated molecular patterns (DAMPs), highly conserved molecular patterns of body’s own structures, hidden under normal conditions become exposed under cellular stresses and damage [14], leading to sterile inflammation, IL1β release and mTOR activation [15].

1.1.1.2 Chaperone-dependent autophagy

In **Chaperone-mediated autophagy (CMA),** no isolation membrane is required. The cargo (only protein, no organelles) is transferred into the lysosome across the transmembrane lysosomal protein Lamp2A [16]. This is mediated through a cytoplasmatic heat shock protein complex (HSPC, consisting of HSC70 and cochaperons) which recognizes and binds a KFERQ-motif in proteins and is normally covered by an intact tertiary structure of the protein and exposed in damaged proteins [17]. HSPC transports its cargo near lysosomes by using Lamp2A as a receptor. After binding of HSC70 to Lamp2A, Lamp2A forms a multimeric complex allowing translocation for the protein. By that time, HSC70 is already dissociated from Lamp2A and the cargo, the lyHsc70 and Lamp2A multimer perform the translocation of the unfolded protein. Inside the lysosome, lyHsc70 binds to KFERQ and ‚pulls' the protein inside, Figure 1-5. The prevention of protein aggregation during this is essential, as aggregated proteins which cannot be unfolded again cannot pass the lysosomal membrane. Therefore CMA cannot degrade cytoplasmatic protein aggregates like macroautophagy, but it contributes to avoid aggregation by elimination of proteins prior to it. Only with intact lyHsc70, the lysosome is competent for CMA. Regulation of lysosomal acidification has impact on the ability for CMA, as lyHsc70 is inoperable without its pH-optimum. Like lyHsc70, the role of Lamp2A in regulation of CMA flux is important. Its synthesis can be increased or its degradation can be decreased to promote CMA. It is interesting to note that Lamp2 is not under direct control of TFEB like other lysosomal proteins [2, 18]. Disruption of CMA convincingly shows its physiological importance, since mutation in Lamp2 gene which leads to the lack of Lamp2 protein, results in Danon's disease, characterized by skeletal and severe cardiac myopathies [19, 20].

The KFERQ-motif[1] is a five aminoacid containing sequence and mediation of its function rather depends on the characteristics of the amino acid residues than on their specific sequence. This motif is represented in approx. 40% of mammal

[1] KFERQ-motif composition: formed out of five amino acids, one of them is always glutamin (Q). The pool for the four remaining amino acids consists of lysine (K), arginine (R), aspartate (D), glutamate (E), isoleucine (I), leucine (L), phenylalanine (F) and valine (V). The motif can be completed in different manners, if some rules are obeyed (only one negatively charged aminoacid and either two positively and one hydrophobic or vice versa [17, 18].

proteins after translation, but CMA can also consume some proteins that contain the motif only as a result of post-translational modification. As aforementioned, the KFERQ-motif is exposed in damaged proteins, but post-translational modifications can also be a tool to regulate targeting proteins for CMA. An autophagy-dependend degradation method engages in this pathway, where ubiquitination mediates conformational change to unmask the KFERQ-motif [16-18].

Like macroautophagy, CMA provides amino acids to facilitate cellular adaption under conditions of stress. It is commonly accepted that different autophagy pathways and mechanisms run simultaneously and work synergistically [18].

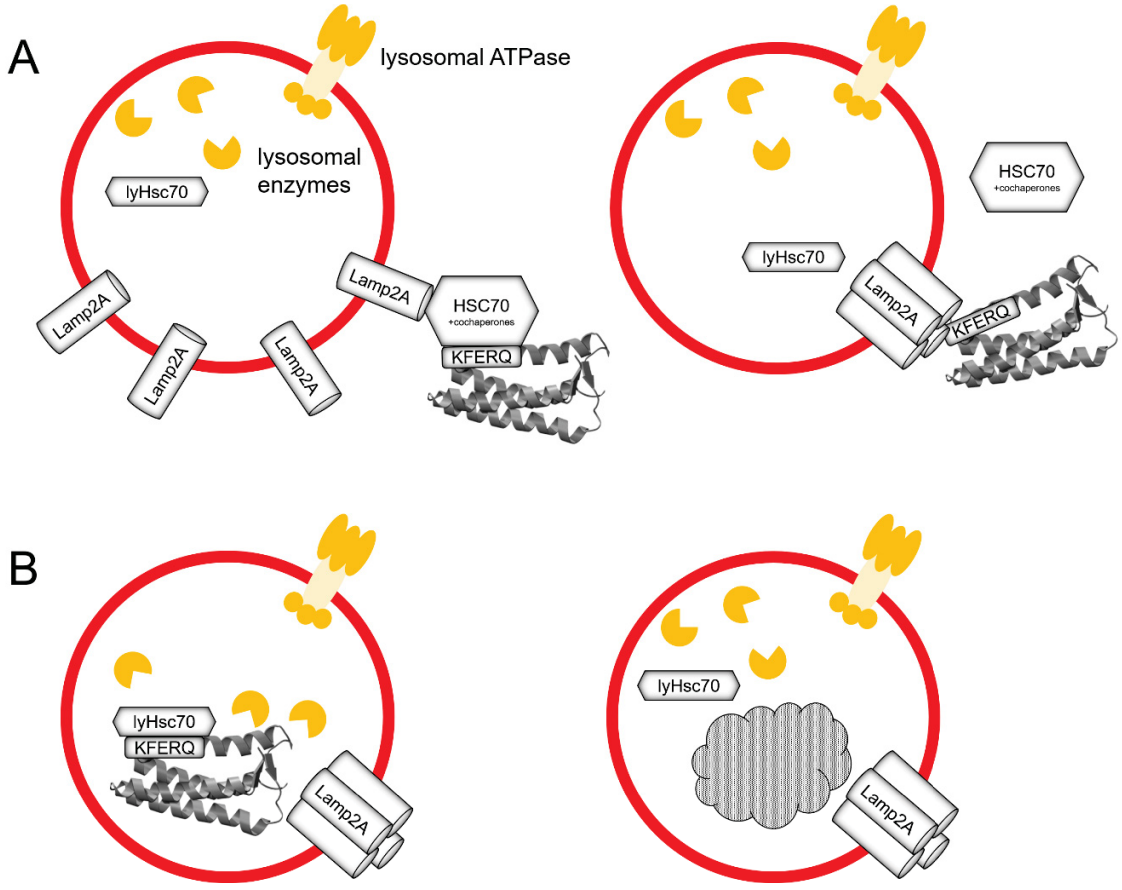

Figure 1-5: Cargo uptake in CMA: [A] Binding of HSC70 to Lamp2A in lysosomal membrane induces formation of multimeric Lamp2A complex serving as channel for cargo uptake. HSC70 early dissociates from Lamp2A and the KFERQ motif. [B] As soon as the Lamp2A channel is formed, translocation of the cargo protein especially due to lyHsc70 pulling it inside, followed by degradation.

Chaperone-assisted selective autophagy (CASA) is a form of macroautophagy which degrades ubiquitinated organelles and proteins without binding to KFERQ and protein unfolding, but still includes chaperons [18]. HSC70 binds to cargo and with aid of distinct cochaperons, the cargo can be ubiquitinated in a manner recognized by the adaptor p62 in macroautophagy. Main CASA substrates are large proteins (or complexes), e.g. filamin in striated muscle cells. It is an anchor for actin, located at the Z-disc, to maintain connection to integrins in myocyte membrane. During every contraction cycling, this filamin anchor experiences unfolding and refolding, leading to erosion and finally loss of structure and function. CASA is important to maintain muscle contraction by clearance of filamin and defects in CASA can lead to cardiomyopathy and muscle dystrophy like conditions [16].

1.1.1.3 Microautophagy

In microautophagy, no isolation membrane is required. In yeasts for example, the lysosome itself takes up cytoplasmatic cargo by invagination of its own membrane [2]. In mammals, microautophagy occurs as a result of a slightly different mechanism and is called **endosomal microautophagy** (**eMI)** [18]. This is in line with the observation that unlike macroautophagic genes, which are conserved in yeasts and mammals, microautophagic genes are not conserved in mammals. A late endosome (part of endosomal-lysosomal system[2]) takes up proteins by invagination of its own membrane. An endosome with these cargo-containing constrictions inside is called a multivesicular body (MVB). The recognition and recruitment of ubiquitinated cargo proteins to the endosomal membrane is performed by the endosomal-sorting-complexes-required-for-transport (ESCRT). Like macroautophagy, microautophagy and eMI can occur unselectively and selectively. Binding to the KFERQ motif of proteins is rather optional than necessary. However, it can mediate specific degradation, again in concert with HSC70. Interestingly, there is no Lamp2A in endosomal membranes, and HSC70 binds directly to the endosomal membrane. So the protein does not have to pass a narrow channel structure like Lamp2A, allowing also aggegated proteins to be degraded in this pathway. It is not yet determined whether HSC70 is primary bound to endosomes and then ‚catches' its cargo or if it primary binds its cargo and secondly binds to the endosome [16].

[2] Early endosomes serve as a sorting plant for the delivered cargo from endocytosis and autophagy vesicles. They are formed by fusion of smaller vesicles, but also origination from Golgi apparatus is described. Early endosomes can ditsribute their content to recycling endosomes (which mediate transport back to plasmamembrane, e.g. in recycling of surface receptors) or back to the Golgi network. They also send cargo to preformed late endosomes for degradation or mature self into late endosomes. As the late endosome contains more intraluminal vesicles, it is also called multivesicular body. A late endosome fuses with lysosomes in order to degrade the cargo [12, 17].

1.1.2 Benefits of autophagy

In autophagy, the cell digests parts of its own intracellular portions. This can take place to eliminate degenerative proteins, fight against invaded microorganism or eliminate worn out organelles in order to renew them afterwards. The latter is especially important in post-mitotic cells, which cannot renew themselves through cellular division, but completely depend on sorting out and replacing dysfunctional cell organelles (quality control) [2, 21]. This will be elucidated in more detail in the chapter dedicated to mitophagy, the autophagy of mitochondria.

Another interesting aspect to autophagy benefits is its important role in stress physiology. Cells exposed to stress may suffer from limitation of essential resources and therefore experience ATP depletion and disturbance in cellular homeostasis. Cells can survive these detrimental conditions for a short time period, depending on how efficiently it can adapt its own metabolism. In this context, autophagy can serve as a nutrient provider by degradation of cellular proteins, which are dispensable at the moment. Inside the autophagolysosome, the cargo is disassembled into its basic building blocks. If cellular proteins form the cargo, amino acids will be released and will be provided to the starving cell. There are two major possibilities for the recycled amino acids to be of a good use. First, they may be directed toward ATP production, as the tricarboxylic acid cycle can utilize some amino acids after they are transformed into its metabolic intermediates [2, 22, 23]. Second, the amino acids are used for biosynthesis of proteins intended to adapt the metabolism and establish a new bioenergetic homeostasis. Furthermore, since proteins do not represent all of the autophagic cargo, also fatty acids (out of digested lipid droplets or membranes) are released and may serve for ATP production (e.g. in beta oxidation of fatty acids) [2].

1.1.3 Exsessive autophagy and autosis

Cell death through autophagy is called autosis, and it is crucial to distinguish whether a cell died due to autophagy *per se* or due to other reasons with simply upregulated autophagy machinery [24, 25]. Autophagy seems to be an important survival mechanism, as described in the previous chapter. Nonetheless, under some conditions, autophagy may be more harmful than beneficial. Previous experimental data show ambiguous findings, in which autophagy downregulation is linked to the organelle dysfunction and autophagy upregulation was associated with adverse remodelling and even cell death. For instance, in mice subjected to pathological cardiac stress (thoracic aortic banding), cardiomyocyte-restricted Beclin1-overexpressing group showed lesser autopagy-induction than the group with Beclin1 haploinsufficiency. But the restrained activation of autophagy lead to lower degree of adverse remodelling and progression to heart failure than the unrestrained and reinforced autophagy activation in Beclin1 overexpression. In contrast, Atg5 inactivation to disrupt autophagy leads to rapid onset of heart failure [26, 27]. Liu, Y. *et al.* (2013) described autosis as a cell death pathway discrete from apoptosis and necroptosis[3]. As autophagy inductor, they used the cell membrane penetrating peptide Tat-Beclin1 (and as negative control the protein Tat-Scrambled). The induction of autophagy was investigated by western blotting, showing decreased levels of p62 and increased levels of LC3-II in cells treated with Tat-Beclin1. They found that in high concentration and exposure time, Beclin1 was competent to induce cell death and no markers of apoptosis or necroptosis were detected [25, 28]. Also, it is interesting to see that the anti-tumor drug doxorubicin, which is well-known for its cardiotoxicity, highly induces autophagy [29].

It is becoming increasingly apparent that the overall settings determine whether autophagy serves as a survival mechanism or is a harmful process. According to Lavandero, S. et al. (2015) maladaptive autophagy is harmful for cardiomyocytes, regardless of the direction. Excessive upregulation seems to be just as harmful as its severe downregulation [26].

[3] Necroptosis is, like apoptosis, a regulated form of cell death, and thereby distinguishes itself from necrosis [28].

1.1.4 Mitophagy

Mitophagy is the selective degredation of damaged or stressed mitochondria by autophagy [30].

Type 1 mitophagy usually follows mitochondrial fission and it is commonly the result of nutrient deprivation. The process requires an isolation membrane, mediated by Beclin1 and PI3K-complex. The isolation membrane grows and engulfs a whole mitochondrium or a portion of a mitochondrial association which leads to mitochondrial permeability transition (MPT) depolarisation of mitochondrial membrane and its degradation [31].

Type 2 mitophagy is independent of PI3K-complex, and occurs when mitochondria are damaged and their membrane is already depolarized prior to engulfment. LC3-containing membranes now decorate the mitochondrial surface and fuse into a whole structure, encircling the whole mitochondrium, therefore no fission is needed, while **Pink1** and **Parkin** are known to mediate the process [31]. Under normal conditions (in the absence of mitochondrial damage), Pink1 is translocated from the cytosol into the mitochondrial matrix via transport systems TOM and TIM (translocate of the outer/inner mitochondrial membrane). There, it is decomposed by PARL (presenilins-associated rhomboid-like protein, located in the inner mitochondrial membrane), Figure 1-6 A. In mitochondrial stress or damage, the Pink1 mitochondrial import is interrupted and it accumulates in the outer mitochondrial membrane and phosphorylates outer mitochondrial membrane proteins like Mfn2 (mitofusin1/2) and cytosolic ubiquitinin. Cytosolic Parkin, an E3 ubiquitin ligase, is attracted by Pink1 phosphorylated proteins and flags mitochondria for mitophagy by ubiquitinating them with Pink1-phosphorylated ubiquitn (explanation for Parkin selectivity to not ubiquitinae other cytosolic proteins), Figure 1-6 B [32, 33]. As described, p62 operates as an adaptor for ubiquitinated cargo due to its interaction with LC3-II in the isolation membrane, allowing the isolation membrane to find the ubiquitinated mitochondrium [2]. This pathway is considered to be of importance in stressed myocardium, since Parkin ablation does merely alter basal heart function under normal conditions, but under conditions of pathological stress (e.g. after myocardial ischemia), cardiac recovery is impeded due to impaired mitochondrial clearance [32, 33]. Parkin translocation to mitochondria is inhibited by p53 [13, 34].

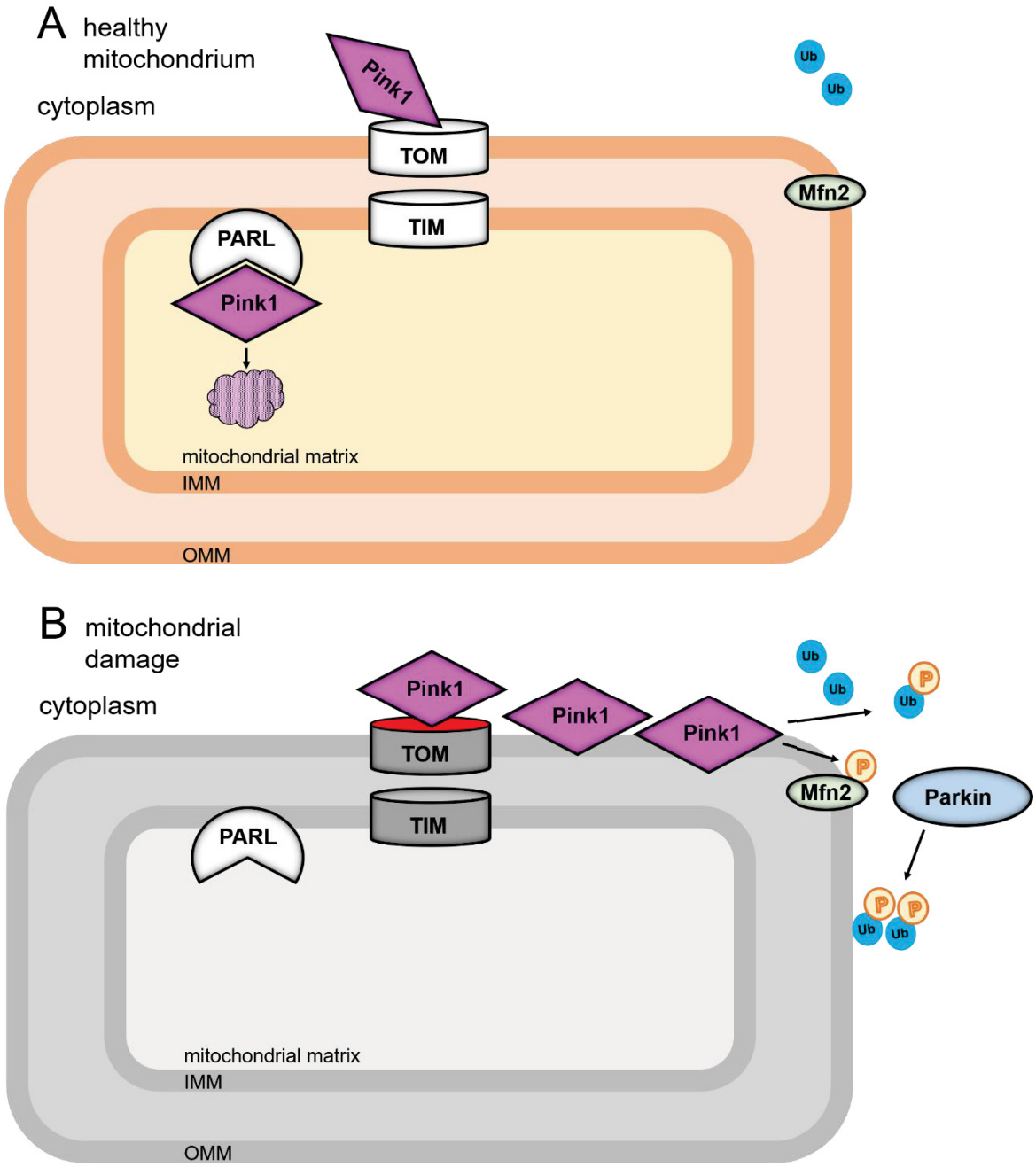

Figure 1-6: Pink1 and Parkin dependent mitophagy. [A] Under normal conditions, Pink1 is constitutively imported into mitochondria and therefore cytopasmatic levels are very low. Followed by degradation by PARL in the inner of the mitochondrium. [B] In mitochondrial damage, mitochondrial Pink1 import is disrupted, leading to Parkin attraction via phosphorylation of mitochondrial Mfn2. Parkin marks damaged mitochondrium for mitophagy with Pink1-phosphorylated ubiquitin. Inspired by Dorn, G. W. [32].

Type 3 mitophagy (micromitophagy) is a sort of microautophagy, with degradation of mitochondrial fragments and is independent of Atg5 and LC3, but it is also dependent on Pink1 and Parkin [34]. Mitochondrial derived vesicles which bud off damaged mitochondria (no fission or depolarization) contain many oxidized mitochondrial proteins and are uptaken by lysosomes. Their production is enhanced in conditions of oxidative stress and by damaged mitochondria [31].

1.1.5 Autophagy/Mitophagy in cardiomyocytes

Cardiomyocytes are postmitotic cells, which means they are matured and terminally differentiated and no longer capable of undergoing mitosis. Autophagy is discussed to play a crucial role in quality control of cellular homeostasis of cardiomyocytes, including both nonselective and selective autophagy like mitophagy [2]. Especially in the heart, as a continuously working muscle, high functionality of mitochondria has to be guaranteed in order to provide the huge amounts of ATP needed, approx. 6kg per day [13]. Effective clearance of worn-out mitochondria is coupled to biogenesis of new mitochondria and the homeostasis of those two processes is essential for healthy cardiac physiology. Consequently, in recent years, the impairment of autophagy has been causally linked to cardiac dysfunction and the development of heart failure [31].

1.2 Heart failure

Heart failure is a clinical syndrome with different possible underlying pathologies. Clinical cardinal signs are among others edema, fatigue and dyspnea. Etiologically, there are plenty of causes for heart failure (e.g. mycardial infarction, hypertension, valve disease, arrhythmia, cardiomyopathies, congenital heart failure, infective causes, drug induced damage, infiltrational conditions like amyloidosis, sarcoidosis and neoplasia, storage disorders like haemochromatosis or glycogen storage disease, and metabolic diseases). Abnormal levels of natriuretic petides (elevated NTproBNP or BNP) indicate heart failure and classification is based on LVEF measurement, commonly performed by echocardiography. **HFrEF** (**heart failure with reduced ejection fraction** due to poor pumping function/impaired contractility) is diagnosed, if LVEF is below 40%. Diagnostic of **HFpEF** (**heart failure with preserved ejection fraction** due to poor ventricular filling because of reduced relaxability/myocardial thickening and stiffening) remains troubling, there are several score-based algorithms, but a more simple practical assessment exists to confirm HFpEF (e.g. : LA size > 32 mL/m2, mitral E velocity > 90cm/s, septal e‘ velocity < 9cm/s, E/e‘ ratio >9) [35]. The American College of Cardiology recently supplemented this classification with an „Universal Definition and Classification of Heart Failure“, where they, among others, further distinguished symptomatic heart failure according to left ventricular ejection fraction (EF) into the following stages:

- HFrEF LVEF ≤ 40% (heart failure with reduced EF)
- HFmrEF LVEF 41-49% (heart failure with mildly reduced EF)
- HFpEF LVEF ≥ 50% (heart failure with preserved EF)
- HFimpEF LVEF baseline ≤ 40% with ≥ 10 point improvement from baseline resulting in LVEF >40% (heart failure with improved EF)

To note, that a very high EF (> 65-70%) is also suspicious, e.g. for left ventricular shrinkage (e.g. in HCM, amyloidosis) [36].

1.2.1 Heart failure with preserved ejection fraction (HFpEF)

In HFpEF, patients may suffer from similar symptoms like in HFrEF, but in this case EF is not reduced. A hallmark of HFpEF is abnormal relaxation and left ventricular filling in diastole, causing elevation in left venticular filling pressures, in early stages only under exercise and in late stages also under resting conditions. Diastolic refillment is impaired due to increase in myocardial wall stiffness (stiffening of myocytes and/or deposit of extracellular collagen) or decrease in relaxation abilities. Especially the inability to adapt and shorten relaxation time when heart frequency is increasing. This leads to increase in left ventricular filling pressures and forces the left atrium to undergo remodelling in order to compensate for the impaired passive filling ability and force volume into the left ventricle by active contraction. But as soon as left atrial function declines or decompensates, adverse effects expand onto lung vessels and the right heart. By now, the phenotype of cardiac remodelling is not simply reduced to concentric left ventricular hypertrophy anymore. In fact, HFpEF can present with different phenotypes, varying in dimension of hypertrophy and proportion of chamber to wall thickness. And only noted at the margins, per definition EF is normal, which does not mean that overall systolic function is normal [37]. In HFpEF, cardiomyocytes are decreasing in number and are increasing in size, apoptosis rate and fibrosis, which are normal changes coming with age, but they can be perpetuated by comorbidities like diabetes or hypertension, leading to heart failure. In age, there is a raise in (myo)fibroblast activity, also caused by higher ROS levels. Since autophagy declines with age, dysfunctional mitochondria accumulate and tend to release ROS [38]. To mention again myocardial stiffness, it is reported that in HFpEF abnormalities in the titin protein were found. Titin spans through the sarcomere and holds properties like an elastic spring. It is responsible for the strechability and respectively stiffness of cardiomyocytes, and the adjustment of its compliance is achieved by post-translational phosphorylation. In HFpEF hypophosphorylated titin can be found, with increase in its resting tension. This titin-related pathologies affect the passive relaxation abilities [38, 39]. Then again, the active relaxation abilities are highly dependent on calcium signaling. In diastole, cytoplasmatic calcium levels have to be restored. SERCA2a channels calcium back into the sarcoplasmatic reticulum and NCX1 pumps calcium back to the extracellular space (in interplay with phospholamban and Ca^{2+}/calmodulin-dependent protein

kinase). In HFpEF, calcium handling is disturbed, leading to delayed calcium decay, which hampers active relaxation [38].

Regarding autophagy markers, Hahn, V. S. et al. (2021) performed RNA-analysis on human right ventricular tissue from patients which met criteria for HFpEF. Regarding autophagy, they summarized from their results, that there is an HFpEF-related downregulation of autophagic gene expression [40].

1.2.2 Dilated cardiomyopathy (DCM)

There are different classifications of cardiomyopathies, a very common one is the classification according to their functional phenotypes, e.g. hypertrophied, arrhythmogenic right ventricular, restrictive and dilated cardiomyopathy. According to the American Heart Association, dilated cardiomyopathy (DCM) is a heterogeneous spectrum of myocardial disorders rather than one specified condition, which makes it difficult to define a distinct etiology. It distinguishes oneself with ventricular dilation (usually left ventricle dilated, but encroaching on right ventricle is possible) and impaired systolic function (HFrEF) in the absence of another disease-mediated myopathy (like hypertension, valvular malformation, ischemia etc.) Basically, DCM can become manifest at any age, but there is a peak in the thirtieth to fortieth years of life. When a patient presents with reduced EF, an initial diagnostic workup should rule out ischemic causes and other myocardial diseases. If no criteria for the latter ones are fulfilled, DCM is among the possible differential diagnoses [41]. As mentioned above, DCM presents with reduced left ventricular EF, which often worsens over time. The AHA states, that the prevalence is probably underestimated, and the ACC complements that 1 in 250 people might be affected [42]. DCM can be diagnosed by echocardiography. The left ventricular end-diastolic diameter has to exceed 117 % (of an individual predicted value) and the EF should be less than 45%. Like other cardiomyopathies, DCM can be further differentiated into familial and non familial subgroups. Family history should be taken for at least three generations. If two or more members are affected (or less if at least one died of unexplained sudden cardiac death under the age of 35) familial DCM can be diagnosed [43].

Since there is a familial form, this indicates that there is a genetic component, which can occur heredity or spontaneous. There are more than 60 genes identified, which could participate in the pathogenesis of DCM [42]. To mention only a fraction of proteins affected by genetics: β-myosine heavy chain, α-tropomyosin, cardiac troponin T, laminin A/C, desmoplakin, filamin C, metavinculin, desmin. Most important in the end, in up to 25% of DCM patients, a mutation in the titin gene is found [43].

1.2.3 Autophagy in heart failure

Abdellatif, M. et al. (2020) pictured the dynamics of autophagy in HFrEF. In an animal model, when HFrEF is induced by pressure overload, autophagy seemed to be upregulated. But after observation over a longer time period, autophagy activity declined significantly, in accordance with the notion that autophagy is temporarily upregulated in stressed myocardium to maintain homeostasis, but becomes maladaptive and finally decreases with proceeding adverse cardiac remodelling. Administration of TAT-Beclin1 (autophagy activator) is able to attenuate this adverse cardiac remodelling. This rescue is failing in case of animals with induced autophagy deficiency. Also in HFpEF induced in Dahl salt-sensitive rats, autophagy activators (in this case spermidine) showed cardioprotective effects [19]. Caragnano, A. et al. (2019) investigated the role of sterile inflammation and autophagy in DCM in human hearts explanted from DCM patients with NHYA III or IV. They were compared to hearts from patients after death without DCM. Properties of DCM cardiomyocytes were, among others, the accumulation of aggregated misfolded proteins. Those aggregates failed to induce their autophagical consumption, therefore they were organized as aggresomes [15]. Aggregasomes form in case of overwhelmed protein clearance, aiming to store misfolded proteins in encagements of intermediate cell filaments [44]. Correlating with other literature [45], they found protein aggregats within the cells. The DCM tissue was positive for signs of sterile inflammation. They stated, that DAMPs might trigger IL1β release by inflammasomes, which triggers mTOR [15]. Aleksova, A. et al. (2017) monitored 156 patients with idiopathic DCM for just over seven years. They concluded, that IL1β may be useful for long term prediction of their outcome and mortality [46]. Another important trigger in the DCM tissue are ROS. There is an interplay between ROS, pushing mitochondrial damage forward and in return this again increases ROS, also activating mTOR. All together, they suggested, that mTOR activation in DCM is associated with disruption of autophagy and mitochondrial dysfunction. The depressing effects of mTOR onto autophagy have been discussed previously. Since macroautophagy was not triggered properly, p62 and dysfunctional mitochondria also aggregated. The dysfunctional mitochondria were positive for increased levels of Parkin, correlating with western blot analysis [15].

1.3 Aims and objectives, project description

This thesis aims to investigate, if there is an alteration of selected autophagy markers in tissue homogenates of left ventricular myocardium by quantitative western blot analysis. Dahl salt-sensitive rats in early and late state of hypertension-induced cardiac remodeling will serve as a model for diastolic dysfunction (in early state) and HFpEF (in late state). Further, tissue from human hearts with diastolic dysfunction and DCM will be investigated, with the following overall specific aims:

- To identify potential progressive alterations in autophagic markers over the course of hypertension-induced cardiac remodeling in rat animal model
- To identify common and specific alterations in autophagic markers in human hearts with diastolic dysfunction and DCM
- To identify trans-species alterations in autophagic markers associated with diastolic dysfunction

2 Material and Methods

2.1 Heart failure and autophagy markers

Markers of heart failure

A molecular hallmark of heart failure is the dysregulation of the following proteins: **SERCA2a,** typically its activity and expression is reduced, and **NCX1** with increased activity and expression in the plasma membrane [47].

Markers of autophagy

LC3-II is indicating formation of matured autophagosomes [48]. Typically, increased autophagy would correspond to the decrease in **LC3-I** and increase in LC3-II (and increase in **LC3-II to LC3-I ratio**) due to rapid conversion of LC3-I to LC3-II [49]. More detailed implementations in chapter 4.2.

p62 is degraded in the process of autophagy (in case of autophagy mechanisms depending on p62). Higher levels of p62 are detected when autophagy is inhibited [49, 50].

Atg5 is essential for the formation of Atg12-5-16L conjugate and ist reduction could be interpreted as reduction in autophagic processes. It can be detected as free Atg5 or Atg5-Atg12conjugate [49]. Often, Atg5 deficient animal models are used to show the effects of the autophagy disruption. For example, mice with cardiomyocyte specific deletion of Atg5 develop left ventricular hypertrophy, finally causing dilated heart failure and mitochondrial dysfunction [51].

Pink1 and **Parkin** levels in western blot typically correlate with mitophagy activity. Given the ubiquitary presence of Parkin in cells, the detection of total-Parkin should ideally be complemented by detection of mito-Parkin and cyto-Parkin [52].

mTOR is a potent inhibitor of autophagy. Upregulation of mTOR levels, in particular of its activated form, phospho-mTOR, is typically indicative of reduced autophagy [49, 53].

2.2 Animal model for hypertensive cardiomyopathy

Every procedure involving animals adhered to the Federal Act on the Protection of Animals (Medical University of Graz) and was approved by the Institutional Animal Care and Use Committee.

Dahl salt-sensitive rats are an established inbred strain serving as model for hypertension and cardiac remodelling, as they rapidly develop hypertension if put on HSD. As normotensive controls, either Dahl salt-resistant rats on HSD or Dahl salt-sensitive rats on LSD can be used [Anderson, P. G., Bishop, S. P. and Peterson, J. T. (2006a)]. For the purpose of this study, male Dahl salt-sensitive rats were purchased from Charles River Laboratory (Boston, USA) at 5 weeks of age. When they reached 7 weeks of age, baseline *in vivo* phenotyping was performed and they were put on respective diets. A subgroup was fed a HSD (8% NaCl, purchased from Research Diets, formula D05032408Y). The control subgroup was fed a LSD (0.3% NaCl, purchased from Research Diets, formula D10001R). After 5 weeks on the respective diet (early stage of cardiac remodelling), *in vivo* phenotyping was performed and a portion of the animals was sacrificed (LSD and HSD early, euthanasia and cervical dislocation) to collect organs. The remaining rats (HSD only) continued their diet for further 5 weeks (HSD late, representing the late stage of cardiac remodelling), again *in vivo* phenotyping was performed followed by sacrifice and gravimetric measurements.

In vivo phenotyping included biweekly tail cuff blood pressure measurements (performed with CODA® tail cuff system, Kent Scientific Corporation, USA) and transthoracic echocardiography (performed with Vevo 3100 VisualSonics, Toronto, Canada) with rats under light anesthesia (1-1.5% isoflurane and 1.5-2 L/min oxygen flow). For echocardiography, images were acquired in M-mode in parasternal long axis to obtain left ventricular mass (LV). The characterization of *in vivo* phenotype was performed as a part of the ongoing doctoral thesis of Julia Voglhuber, MSc, and is included here with her permission.

2.3 Left ventricular tissue from human hearts

The Ethical Committee of the Medical University of Graz approved the use of human tissue samples, which was carried out in accordance with the *Declaration of Helsinki*. Human tissue from left ventricular myocardium, provided by the clinical department for cardio surgery (Medical University of Graz), was selected from non-failing hearts, hearts with diastolic dysfunction and from failing hearts with DCM. Upon ice-cold cardioplegia, cardiac biopsies were harvested from the left ventricular free wall, quickly frozen in liquid nitrogen and stored at -80°C for future analysis. The patient characteristics are listed in Table 2-1.

Table 2-1: Patient characteristics: NF-non failing, DD-diastolic dysfunction; Data are presented as mean ± S.E.M.

	N	**Age** [a]	**Female** [%]	**BMI**	**EF** [%]	**NTpBNP** [pg/ml]
NF	5	53.6 ± 6.7	40	27.6 ± 2.3	61.2 ± 2.8	253.8 ± 70.3
DD	6	60 ± 3.2	33	27.8 ± 2	62.2 ± 2.2	2110.4 ± 1175.4
DCM	5	46.6 ± 4.8	40	27.1 ± 2.7	26 ± 3.7	2794 ± 852.5

2.4 Immunoblotting

2.4.1 Sample homogenization for protein extraction

Table 2-2: Homogenization buffer for protein extraction and immunoblotting

Reagent	Company	Catalog #	Conc
Glycerol	CarlRoth	3783.1	10%
IGEPAL®CA-630	SigmaAldrich	I8896	1%
NaCl	CarlRoth	3957.1	137mM
Tris-HCL pH 7.4	CarlRoth	8789.2	20mM
NaF	SigmaAldrich	7920	20mM
Sodium pyrophosphate	SigmaAldrich	6422	1mM
ß-Glycerophosphate	FlukaBioChemika	50020	50mM
EDTA pH 8 ethylene-diamin-tetraacetic-acid	SigmaAldrich	EDS	10mM
EGTA pH 7 ethylene-glycol-tetraacetig-acid	SigmaAldrich	E4378	1mM
PMSF phenyl-methyl-sulfonyl-fluoride	CarlRoth	6367.1	1mM
Sodium orthovandate	SigmaAldrich	6508	1mM
Aprotinin	CarlRoth	A162.1	4µg/ml
Leupeptin	SigmaAldrich	L2023	4µg/ml
Pepstatin A	SigmaAldrich	P4265	4µg/ml

Homogenization buffer was prepared with ddH_20 according to Table 2-1 (in that same order). As soon as sodium orthovandate was added, the buffer was protected from light. The tissue pieces were stored at -80°C, fragment collection with pestle and mortar and weighing were performed without thawing (using liquid nitrogen-cooled tools). The tissue amount used was in range of 50-70 mg and ultimately per 10 mg of sample, 100 µl of homogenization buffer were used. The tissue pieces were washed several times with ice-cold PBS (Sigma Aldrich, SLCH5832) in an eppi tube to remove excess blood. Throughout protein extraction, samples were kept on ice. Homogenization buffer was added to tissue pieces in two steps. First, tissue

pieces were minced with scissors and smashed with an electric pistil, followed by centrifugation at 4°C for 3 min at 8000 rpm. The supernatant was transferred into a fresh tube. Then, the second half of the homogenization buffer was added onto the remaining tissue pieces, which were again smashed with an electric pistil and centrifuged briefly in a bench-top centrifuge. The supernatant was combined with the yield from the first round and centrifuged at 4°C for 10 min at 15.000 rpm. The final supernatant was collected into a new tube and snap-frozen in liquid nitrogen before storage at -80°C until further usage. 3 µl of this sample homogenate was put aside and stored separately for protein concentration determination.

2.4.2 BCA assay

Table 2-3: Pierce™BCA assay reagents and material

Reagent	Company	Catalog #
Pierce™ BCA Protein Assay Reagent A	ThermoFischer	23228
Pierce™ BCA Protein Assay Reagent B	ThremoFischer	23224
Pierce™ BSA standard 0-2000 µg/ml	ThermoFischer	23209
Microplate 96 flat-bottomed well plate	GreinerBioOne	655101

Photometric quantification of protein concentration in the sample homogenate was carried out according to the manufacturer's instructions (reagents used see Table 2-3). Therefore, a portion of the sample homogenate was diluted (1:15 with ddH_20). To create a BSA standard curve, nine standards (in µg/ml: 0, 50, 125, 250, 500, 750, 1000, 1500 and 2000) were used. Each sample and standard was run in duplicates. First, 10 µl of sample or standard were transferred to the well plate before 200 µl of BCA working solution (reagent A and B in a 50+1 ratio) were added. The plate was covered and incubated for 30 minutes at 37°C. Photometric measurement of absorbance was carried out with Spectramax Plus 384 microplate reader (Molecular Devices) at 562 nm. The unknown protein concentration of the samples was derived by interpolating into the standard curve.

.

2.4.3 Immunoblotting

Table 2-4: Immunoblotting reagents and material

Reagent	**Company**	**Catalog #**
Tris	CarlRoth	4855.2
NaCl	CarlRoth	3957.1
Tween®20	SigmaAldrich	P1379
Glycine	CarlRoth	0079.3
Methanol	Supelco	1060092511
XT Sample buffer 4x	BioRad	1610791
XT Reducing agent 20x	BioRad	1610792
XT MOPS Running Buffer 20x	BioRad	1610788
Protein Dual Color Standards	BioRad	1610374
Ponceau S solution	SigmaAldrich	P7170-1L
Milk Powder	CarlRoth	T145.2
Bovine Serum Albumin	SigmaAldrich	a7906-50g
Clarity Western ECL substrate	BioRad	170-5060
SuperSignal West Femto	ThermoFischer	34095
Restore WB Stripping Buffer	ThermoFischer	21059
Product	**Company**	**Catalog #**
Criterion XT Precast Gel 4-12% Bis-Tris, 18 Well, 30 µl, 1mm	BioRad	3450124
Nitrocellulose Blotting Membrane 0.45 µm	GEHealthcare	10600002
Criterion blotter Filter paper	BioRad	1704085

Table 2-5: Antibody list: All antibodies were diluted with 0.5% MP/TBST (milk powder in TBST buffer) with exception of LC3B, which was diluted with 0.5% BSA/TBST (bovine serum albumin in TBST buffer)

Primary antibody	**Host**	**Dilution**	**Company**	**Catalog#**
GAPDH	rabbit	1:2000	CellSignaling	5174
p-mTOR (Ser2448)	rabbit	1:750	CellSignaling	2971
mTOR	rabbit	1:1000	CellSignaling	2972
NCX1	rabbit	1:5000	Abcam	177952
Serca2a	rabbit	1:5000	Badrilla	A010-20
p62	rabbit	1:500	SigmaAldrich	P0067
Atg5	rabbit	1:1000	Abcam	108327
LC3B	rabbit	1:1000	CellSignaling	2775
Pink1	mouse	1:200	SantaCruz	517353
Parkin	mouse	1:200	SantaCruz	32282
Secondary antibody	**Host**	**Dilution**	**Company**	**Catalog#**
anti-mouse	sheep	1:5000	GEHealthcare	LNA931V/AH
anti-rabbit	donkey	1:5000	GEHealthcare	NA934V

For immunoblotting 30 µg of sample were used and accordingly diluted with homogenization buffer before a master mix of sample buffer and reducing agent was added (sample buffer and reducing agent in a 5:1 ratio. For all reagents used see Table 7-4). As protein size reference 4 µl of Dual Color standard was used and each pocket holding samples was loaded with 24 µl. Because LC3-II and LC3-I bands appear in small distance, it is important that they remain separately detectable to quantify each of them individually. The use of a gradient gel (like 4-12% Bis-Tris) is therefore recommended. Gel electrophoresis of gradient gels was carried out on ice, using MOPS running buffer. Initial electrophoresis was started at 70 V for 10 min and continued at 120 V until the dye front reached the end of the gel.

Also, the blotting membrane contributes to the success of LC3-II detection. PVDF membranes are recommended over nitrocellulose membranes, because PVDF retains LC3-II better, due to its hydrophobic affinity [48]. For wet transfer ice-cold

Towbin buffer (Tris 25 mM, Glycine 192 mM, Methanol 20%) was prepared and the sandwich cassette pre-assembled and pre-wet in transfer buffer. After assembling the sandwich, proteins were transferred with 0.4 A at 4°C for 2h.

After tank blotting, membranes were stained with Ponceau S for determination of whole protein and as a quality control of transfer. After cutting the membrane into the respective strips, they were washed in water until the background was destained, but bands clearly visible. Photodocumentation was performed using BioRad ChemiDoc MP Imaging System. Subsequently, membranes were blocked in 5% MP/TBST or 5% BSA/TBST for LC3 determination, for 1h at room temperature. After that, the membrane was briefly washed with TBST buffer (Tris-buffered saline with Tween®20, Tris 20 mM, NaCl 137 mM, Tween®20 0.1%)) and subsequently incubated with the respective primary antibody (Table 7-4), at 4°C overnight or at least 2h at room temperature. Membranes were washed three times for 5 min with TBST buffer before incubation with secondary antibodies was performed for 1h at room temperature. Again, membranes were washed three times for 5 min with TBST buffer before incubation with BioRad Clarity Western ECL substrate (incubation time 2 min) and detection with BioRad ChemiDoc MP Imaging System in manual signal accumulation mode. If necessary for following incubation with another antibody, the membrane was exposed to stripping buffer for 5 to 30 min at room temperature, depending on the intensity of the band to be removed. After that, the membrane was washed three times for 5 min with TBST buffer, blocked again for 20 min in 5% MP/TBST, and incubated with BioRad Clarity Western ECL substrate to check if the membrane was ultimately cleared of antibody residue. Then, normal incubation procedure with primary and secondary antibody was resumed. Ultimately, membrane strips were briefly washed in TBST and dried for storage in air-tight foils.

For quantification, the BioRad software Image lab 6.0.1 was used. The signal intensity of each band was quantified by usage of volume tools and manually determining the area of interest (each band) with a rectangle. The adjusted volume values, with global background subtraction method in place, were used for further evaluation. The data were normalized to the corresponding signal of the housekeeping protein GAPDH and to the mean of the respective control group.

2.5 Statisitcal analysis

GraphPad Prism 9 (GraphPad Software, Inc) was used to perform statistical analysis. First, potential outliers were identified by ROUT method with a Q value of 1%. Then, the values were tested for normality of distribution by Shapiro-Wilk-test and D'Agostino-Pearson-test. If normal distribution criteria were fulfilled, one-way ANOVA with Tukey's multiple comparisons test (of each group compared with each other in rats and of each group compared to control in humans) was applied. If normal distribution was violated, Kruskal-Wallis-test with Dunn's multiple comparisons test was performed. $p \leq 0.05$ was considered significant.

3 Results

3.1 *In vivo* characterisation of hypertensive Dahl salt-sensitive rats

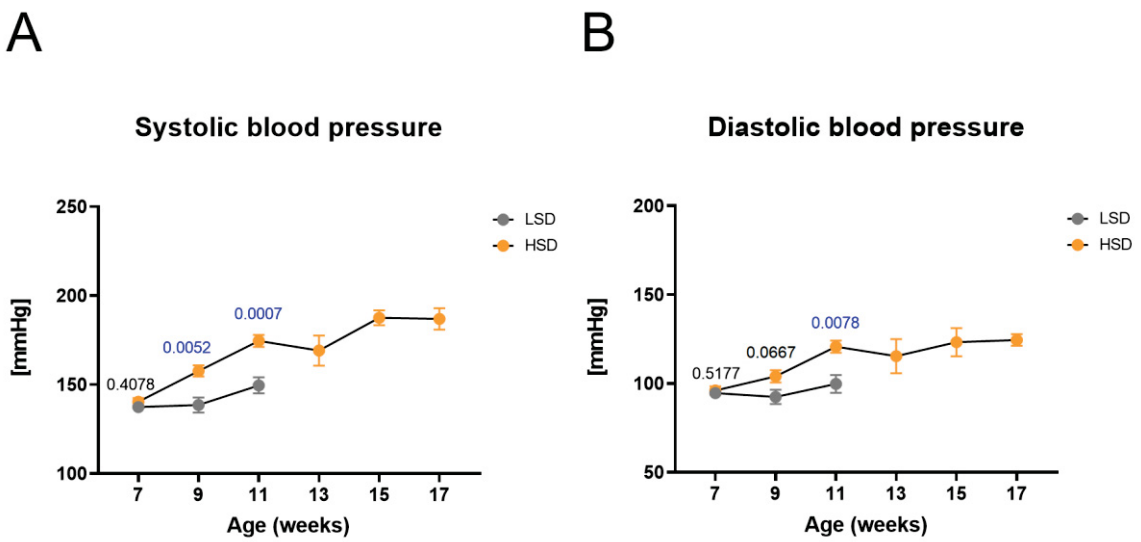

Figure 3-1: Blood pressure measurements of Dahl salt-sensitive rats: Changes in systolic [A] and diastolic [B] blood pressure on respective diets. LSD (n=7), HSD early until week 12 (n=5), HSD late until week 17 (n=3). P<0.05 was considered significant. By courtesy of Holzer, Senka PhD and Voglhuber, Julia MSc.

Before the respective diets, average blood pressure values did not differ between the groups (Figure 3-1; for LSD group 137/95 mmHg and for HSD group 140/96 mmHg). Two weeks after the start of the different diets, in the early timepoint of the HSD group, they already showed significantly increased systolic pressure values (Figure 3-1A; p=0.0052), and the difference to LSD group further grew after four weeks on HSD (p=0.0007). While the control LSD group maintained normal blood pressure values and was not further studied, HSD group was continued and after five more weeks, the average systolic blood pressure in the late timepoint of the HSD group was 187 mmHg. Diastolic blood pressure was increased, yet not significantly different in the early timpepoint of HSD group and it reached statistical significance at week eleven (Figure 3-1B; p=0.0078). The unexpected drop in both systolic and diastolic blood pressure at week 13 was not observed in overall blood pressure values of the whole cohort (see supplements, Figure 7-1) and it is likely an effect of a small sample size used for this diploma thesis.

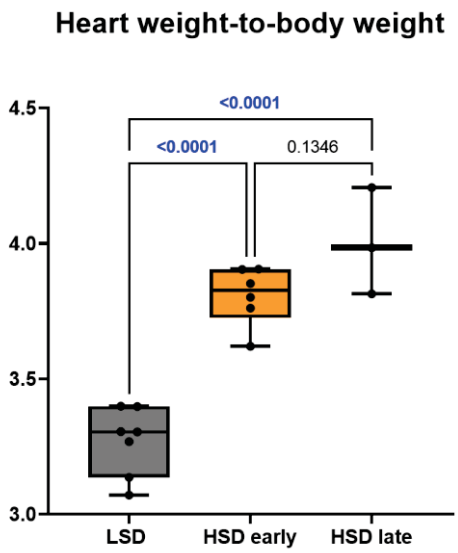

Figure 3-2: Heart weight in Dahl salt-sensitive rats. Changes in heart weight-to-body weight depending on respective diets. LSD (n=7), HSD early until week 13 (n=5), HSD late until week 17 (n=3). P<0.05 was considered significant. By courtesy of Holzer, Senka PhD and Voglhuber, Julia MSc.

When comparing LSD and early timepoint of HSD, it becomes clear that the rats fed HSD showed early a significant increase of their relative heart weight, quantified by the heart weight-to-body weight ratio (Figure 3-2; p<0.0001). When rats on HSD reach late stage of cardiac remodelling, the relative heart weight does not further increase in a significant amount.

3.2 Calcium handling proteins during early and late cardiac remodelling in Dahl salt-sensitive rats

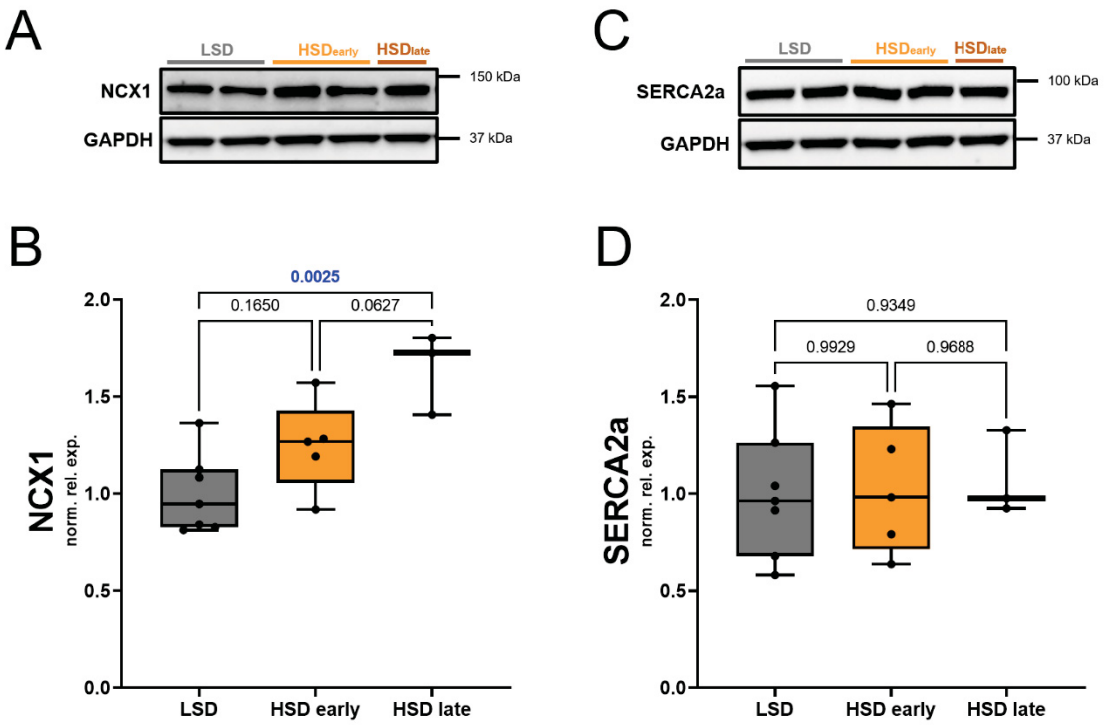

Figure 3-3: Results of calcium handling proteins in Dahl salt-sensitive rats: Western blots and quantitative results. [A, B] NCX1 and [C, D] SERCA2a. P<0.05 was considered significant.

NCX1 and SERCA2a were used as markers for heart failure. In NCX1 analyses, trend toward increase but no significant difference was found between LSD and early-timepoint HSD (Figure 3-3A and B). However, it stood out that in the late stage of cardiac remodelling, rats developed significantly higher NCX1 levels compared the LSD group (Figure 3-3B; p =0.0025).

In contrast, we detected no change in SERCA2a levels between LSD and HSD group at either timepoint studied (Figure 3-3C and D).

3.3 Autophagy markers in Dahl salt-sensitive rats in early and late stage of cardiac remodelling

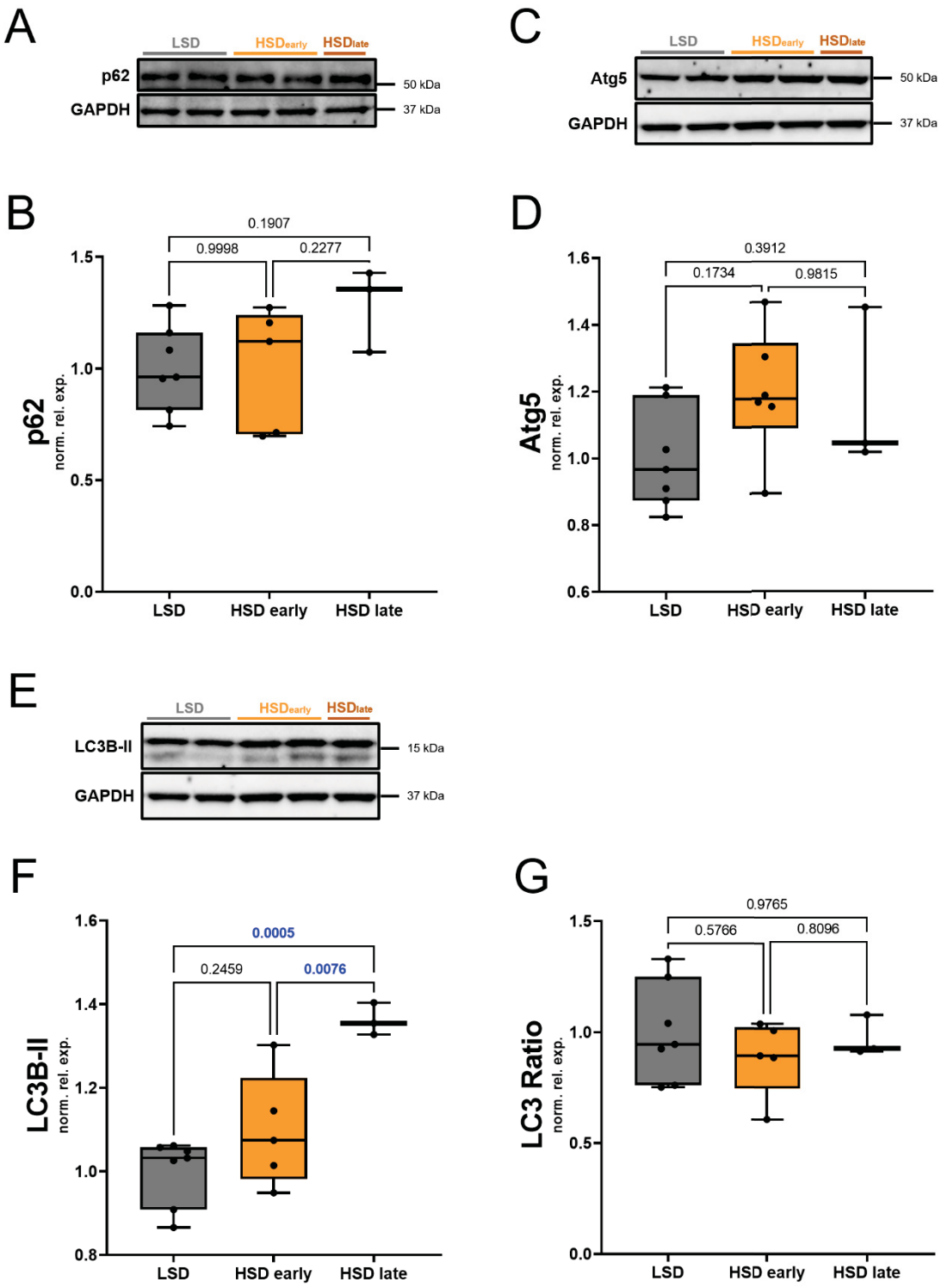

Figure 3-4: Results of autophagy-related proteins in Dahl salt-sensitive rats: Western blots and quantitative results. [A, B] p62, [C, D] Atg5 and [E, F, G] LC3B. P<0.05 was considered significant.

There was no significant alteration of p62 levels between the groups at any assessed timepoint (Figure 3-4A and B). In late timepoint HSD, some rats sowed higher levels of p62 compared to the maximum detected in LSD and early HSD, but due to the small sample size and high variation, the results did not reach the extent for significance (Figure 3-4B).

Results emerging from detecting Atg5 could not prove that the groups differed significantly from each other (Figure 3-4C and D).

When evaluating LC3B-II levels apart, we could show that there is a significant development between the groups (Figure 4-3E and F). While there was very little difference between LSD and early timepoint HSD, the further increase in the late timpeoint HSD and the overall difference between LSD and late timepoint HSD (Figure 4-3F; $p=0.0076$ and $p=0.0005$) is clearly apparent. In contrast, this development could not be confirmed by the LC3 ratio of LC3B-II to LC3B-I, which showed no alteration (Figure 3-4G).

3.4 Autophagy-regulator mTOR in Dahl salt-sensitive rats in early and late stage of cardiac remodelling

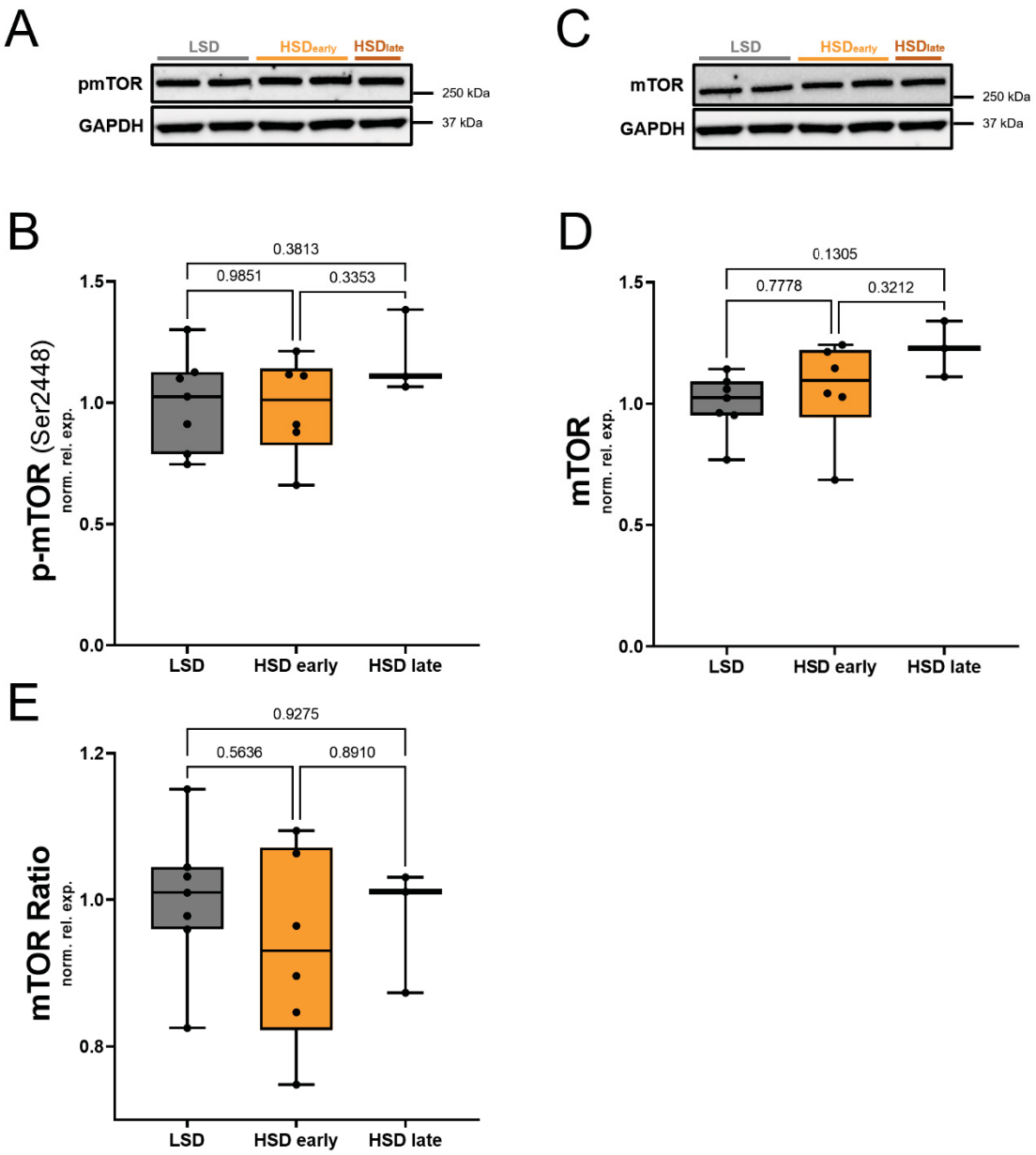

Figure 3-5: Results of mTOR proteins in Dahl salt-sensitive rats: Western blots and quantitative results. [A, B] p-mTOR, [C, D] mTOR and [E] p-mTOR to mTOR ratio $P<0.05$ was considered significant.

In general, our mTOR analyses were not able to show any significant changes between the groups. mTOR phosphorylation in LSD and both timepoints of HSD was virtually unchanged (Figure 3-5 A and B).

Worth noting, however, is that we noticed a slight upward trend in mTOR levels

when comparing early LSD to the late timepoint of HSD, but no significant change was achieved (Figure 3-5C and D).

The ratio of p-mTOR to mTOR again showed no alteration between the groups (Figure 3-5E).

3.5 Mitophagy markers in Dahl salt-sensitive rats in early and late stage of cardiac remodelling

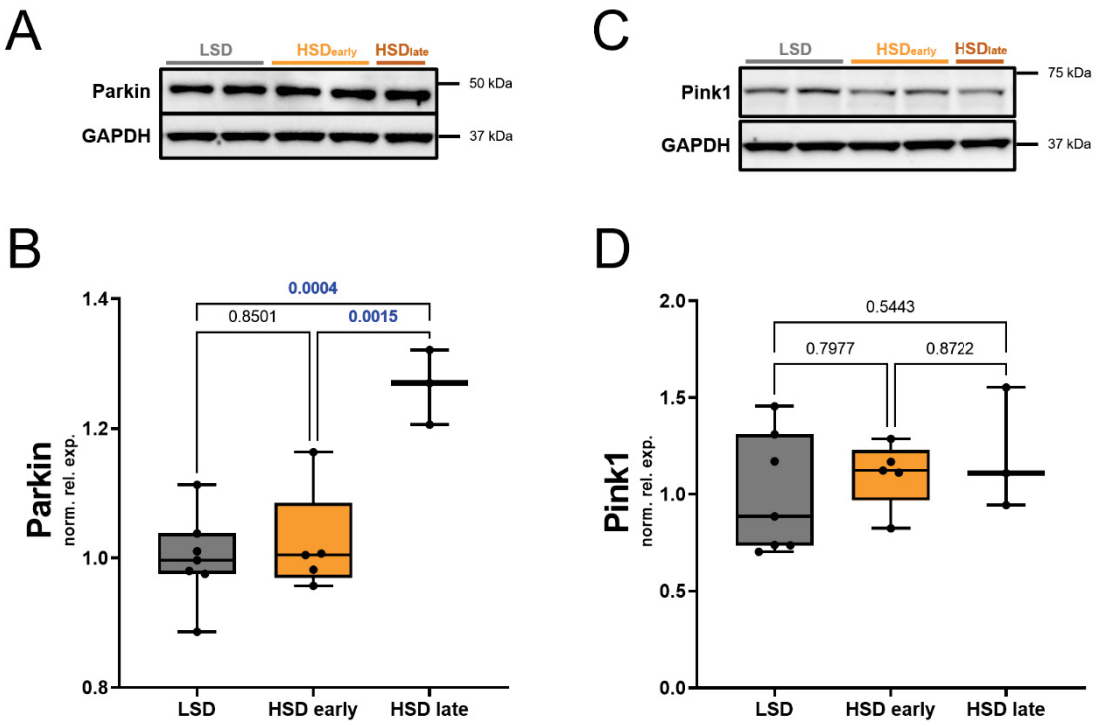

Figure 3-6: Results of mitophagy-related proteins in Dahl salt-sensitive rats: Western blots and quantitative results. [A, B] Parkin and [C, D] Pink1. P<0.05 was considered significant.

When looking at Parkin levels of rats in late stage of cardiac remodellig, the increase in comparison with the other groups is striking (Figure 3-6A and B). Initially, there was no change between LSD and early timepoint HSD group, but was followed by a significant increase in the late timepoint HSD group (Figure 3-6B; p =0.0015).
In contrast, Pink1 showed no significant change in levels between LSD and HSD groups (Figure 3-5C and D).

3.6 Calcium handling proteins in human diastolic dysfunction & dilated cardiomyopathy (DCM) compared to control

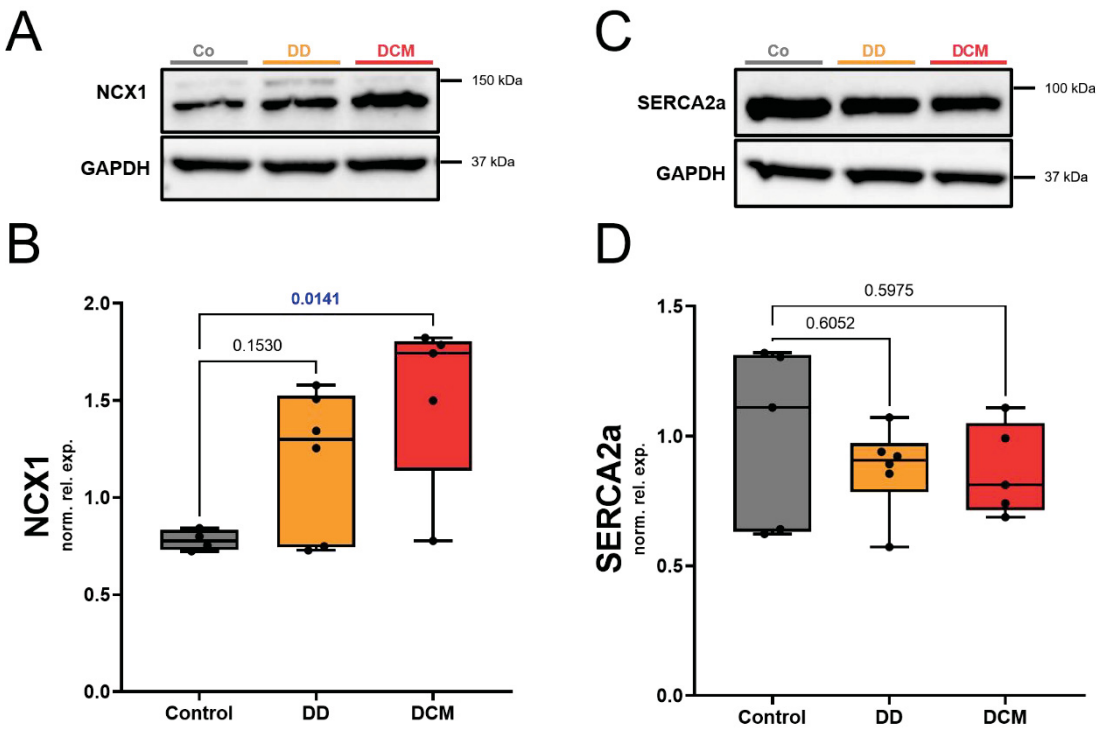

Figure 3-7: **Results of calcium handling proteins in human samples**: Western blots and quantitative results. [A, B] NCX1 and [C, D] SERCA2a in left ventricular myocardium in humans with diastolic dysfunction (DD) and DCM. P<0.05 was considered significant.

Similarly to experiments involving experimental rat model, NCX1 and SERCA2a were used as markers for heart failure in myocardium from patients with increasing degrees of cardiac dysfunction.

There was no significant change of NCX1 levels in diastolic dysfunction compared to control, but there was a strong trend toward elevated levels since single samples had strikingly elevated levels and the minority remained at similar NCX1 levels like in control (Figure 3-7A and B).

Whilst in DCM, a significance in elevation of NCX1 levels, compared to control, was clearly detectable (Figure 3-7A and B; p=0.0141).

SERCA2a levels did not show a significant alteration, neither in diastolic dysfunction nor in DCM, each compared to control. This observation might be dulled due to the inhomogeneity of SERCA2a levels in the control group, with both very high and low

values, aggravating the assessment of levels in diastolic dysfunction and DCM at this sample size (Figure 3-7C and D).

3.7 Autophagy markers in human diastolic dysfunction & dilated cardiomyopathy (DCM) compared to control

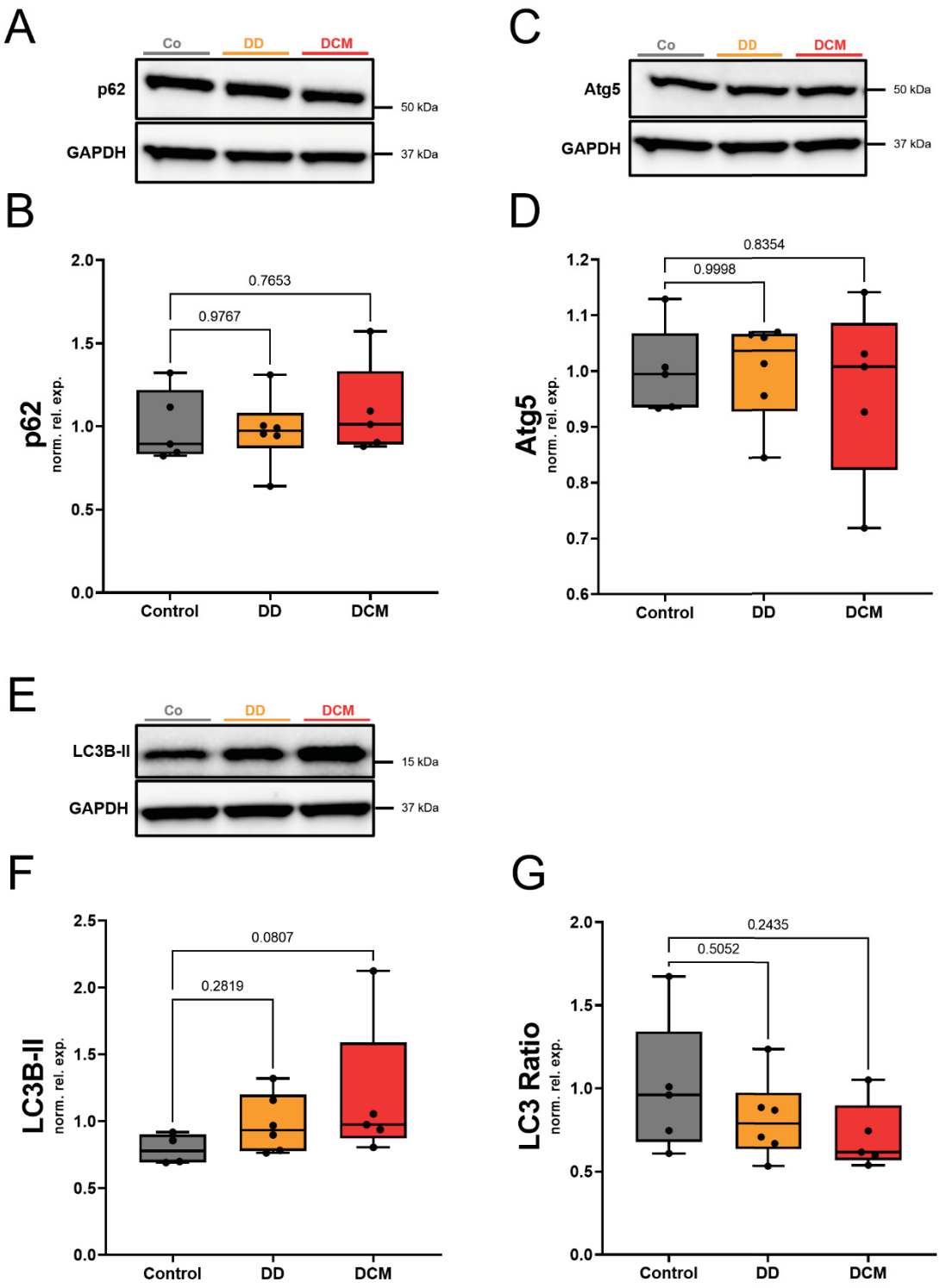

Figure 3-8: Results of autophagy-related proteins in human samples: Western blots and quantitative results. [A, B] p62, [C, D] Atg5 and [E, F, G] LC3B in left ventricular myocardium in humans with diastolic dysfunction (DD) and DCM. P<0.05 was considered significant.

For both p62 and Atg5, we could not detect any noticeable trends or significant changes in diastolic dysfunction or DCM, each compared to control (Figure 3-8). In general, LC3B also showed no significant change between healthy controls and cardiac patients. However, in diastolic dysfunction and DCM, there was a trend toward elevated LC3B-II levels (Figure 3-8E and F), reaching borderline significance in DCM group (Figure 3-8F, $p=0.0807$). LC3 ratio of LC3B-II to LC3B-I, in both groups, showed trends toward reduction, however larger sample number would be needed to (dis)approve the results (Figure 3-8G).

3.8 Autophagy-regulator mTOR in human diastolic dysfunction & dilated cardiomyopathy (DCM) compared to control

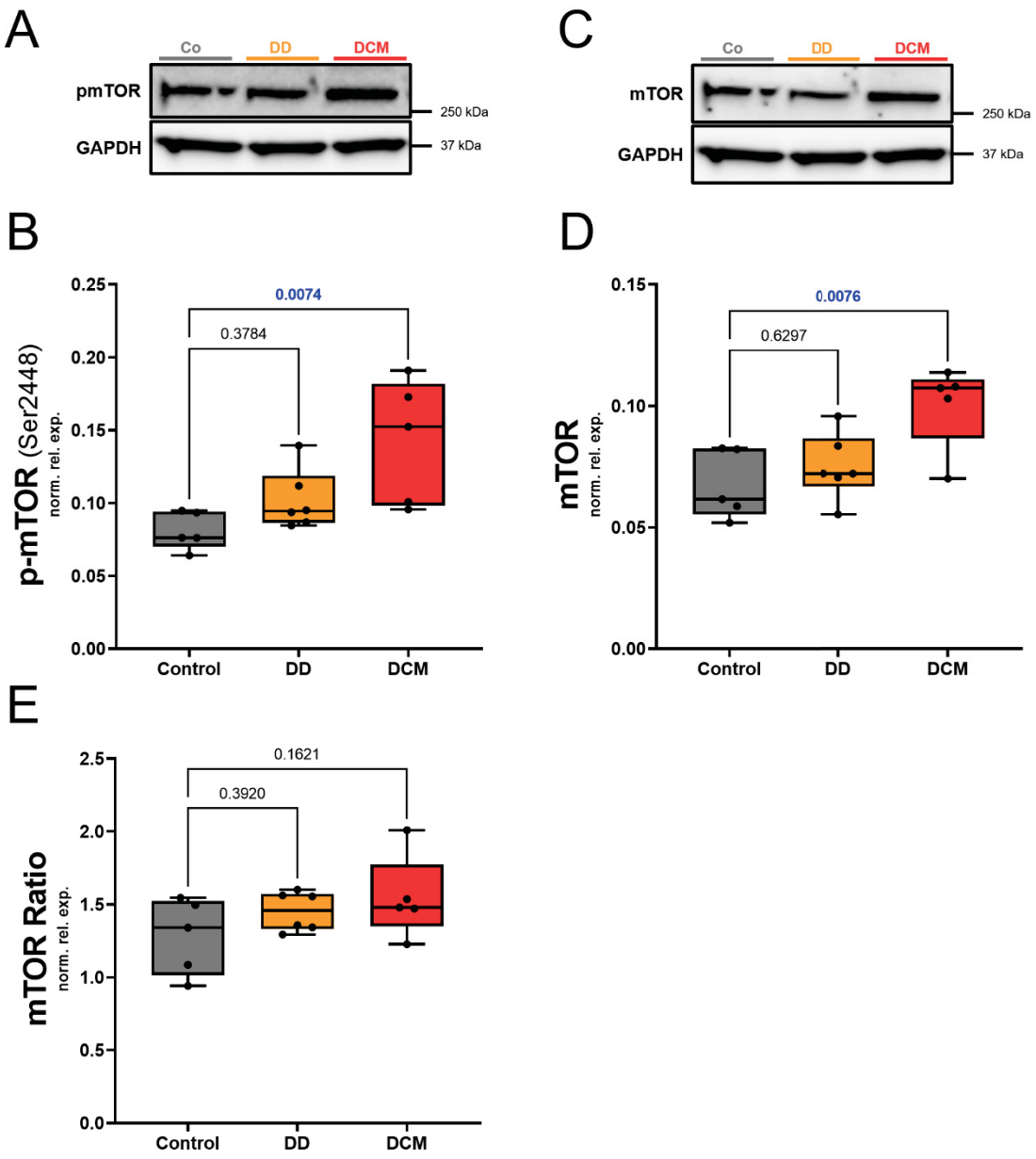

Figure 3-9: Results of mTOR proteins proteins in human samples: Western blots and quantitative results. [A, B] p-mTOR, [C, D] mTOR and [E] p-mTOR to mTOR ratio in left ventricular myocardium in humans with diastolic dysfunction (DD) and DCM. P<0.05 was considered significant.

For diastolic dysfunction, no significant findings in mTOR were detectable, while in DCM the clear disturbance in mTOR signaling was found (Figure 3-9).

p-mTOR and mTOR levels in diastolic dysfunction were slightly but consistently enhanced compared to the control group (Figure 3-9B-E) and larger sample size

would be critical to fully address the potential changes.

In DCM, significantly higher levels of both p-mTOR and mTOR were found, when compared to control (Figure 3-9B; p= 0.0074 and D; p=0.0076). Yet, the formed mTOR ratio did not reach statistical significance in comparison to the control (Figure 3-9E).

3.9 Mitophagy markers in human diastolic dysfunction & dilated cardiomyopathy (DCM) compared to control

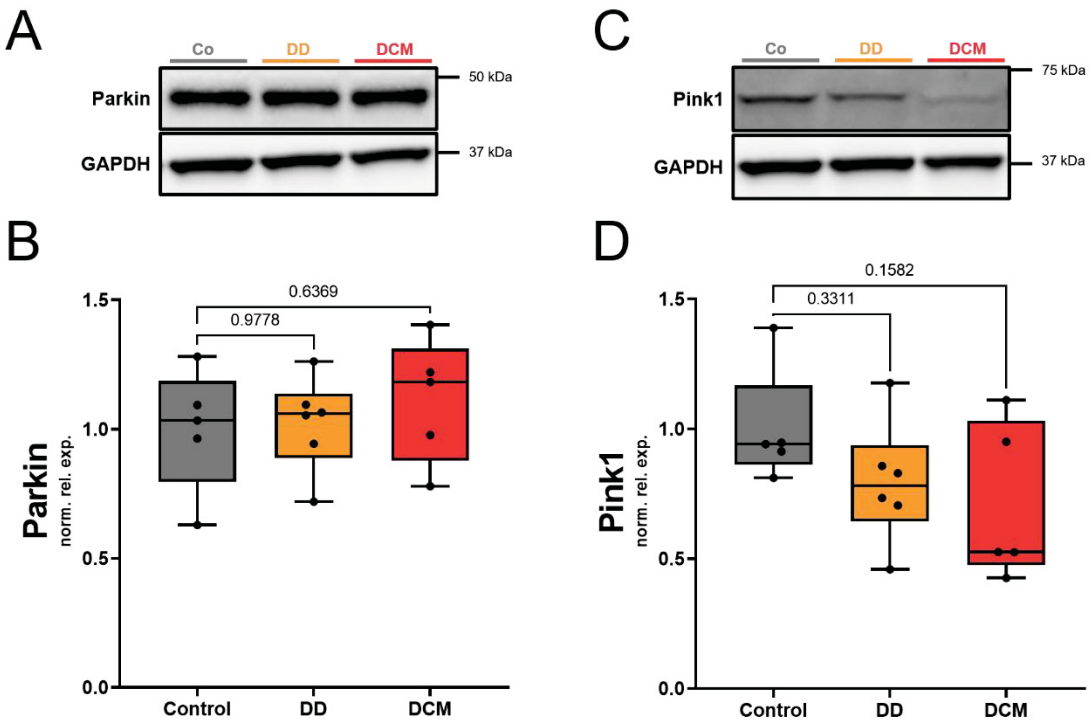

Figure 3-10: Results of calcium handling proteins in human samples: Western blots and quantitative results. [A, B] Parkin and [C, D] Pink1 in left ventricular myocardium in humans with diastolic dysfunction (DD) and DCM. P<0.05 was considered significant.

In this setting, we could not gain a significance in the mitophagy related kinases Parkin and Pink1, however, some differences from control became apparent, in DCM more than in diastolic dysfunction (Figure 3-10).

In diastolic dysfunction, Parkin levels remained unchanged, while single Pink1 values were decreased (Figure 3-10B and D).

In DCM, Parkin remains unchanged as well. But looking at Pink1, the majority of single values is distinguishably decreased in comparison to control, despite no overall reached significance (Figure 3-10D).

4 Discussion

4.1 *In vivo* characterisation of hypertensive in Dahl salt-sensitive rats

Since approximately 50% of the patients with heart failure suffer from HFpEF (population of Europe and USA), Dahl salt-sensitive rats are an important clinically relevant model, commonly used to experimentally mimic HFpEF. However, one should note that only a minority of human heart failing patients with HFpEF suffer this due to hypersaltsensitivity, indicating that comparison with other models would be necessary [54].

The development of hypertension in the HSD group seems to be appropriate for Dahl salt-sensitive rats, since those rats developed comparable blood pressure levels under similar conditions in other studies, too [55].

In this experiment, heart weight-to-body weight is significantly increased in HSD fed rats in comparison to the LSD control (see Figure 3-2), which is a property of hypertensive and failing Dahl salt-sensitive rats (also shown in other experiments [55-57]).

As mentioned before, Dahl salt-sensitive rats were purchased at the age of approximately 5 weeks and were treated equally until they reached an age of 7 weeks. Then they were put on different diets. However, Figure 7-2A in the supplements shows that the body weight differs highly significant between all three cohorts (C), with a mean of 210 g in C1, 241 g in C2 and 284 g in C3 at the age of 7 weeks. As must be expected, these difference in weight are also representative in the rat samples used for this thesis, where rats from C1 had an average weight of 214 g, while it was 228 g in C2 and 288 g in C3 (Figure 7-2B). This may rise the suspicion, that the rats were not the same age at the time of the purchase, and the discrepancy in weight could be explained by a discrepancy in age. This also rises the question, if all rats properly developed diastolic dysfunction and diastolic heart failure or some became hypertensive, only.

4.2 Autophagy in hypertensive in Dahl salt-sensitive rats

Whether all the Dahl salt-sensitive rats developed HFpEF or not, increased NCX1 levels as a hallmark of heart failure indicate that the HSD induced hypertension must have lead to adverse cardiac changes. The missed effect on SERCA2a levels (decreased levels are expected in diastolic heart failure) could be due to the previous mentioned suspicion, that the rats were too old when they were started on HSD and therefore failed to develop complete heart failure.

Few rats in late stage of cardiac remodelling showed slightly increased, yet insignificant levels of p62. If this was an apparent effect in a comprehensive sample size, it would indicate low autophagic activity. The elevated LC3B-II levels, which can be seen in autophagy induction, are the significant finding in this experiment. Atg5 levels showed no change, at large.

To determine the common thread and to square the results which each other, it has to be discussed whether high or low autophagy activity is detected here. As before discussed, elevated LC3-II levels are seen in autophagy induction. But interpretation of LC3 is difficult and comes along with several problems:

First, antibodies against LC3 commonly show less sensitivity for LC3-I, which alters the interpretation of LC3-II to LC3-I ratio. Second, many proteins including LC3, experience transcriptional and post-transcriptional regulation and therefore it is necessary to monitor its mRNA levels simultaneously. Otherwise, it is not possible to differentiate between change in protein level due to autophagy or transcription. Third, LC3-I degrades earlier because it shows higher sensitivity to thawing and freezing cycles. Fourth, the 20S proteasome can degrade LC3-I or turn it into LC3T, which is equally sized like LC3-II in western blot analysis [49]. To sum up, LC3-II levels in western blotting correlate with the number of autophagosomes and do indicate autophagosome formation, but the following turnover is left unconsidered [58]. So this assay would benefit from additional assays to analyze autophagy (e.g. Bafilomycin A1 treatment prior to immunoblotting). Further problems with LC3 as a marker for autophagy are, that LC3 is not required for all forms of autophagy (*see Pink1 and Parkin in mitophagy*). Even though it can serve as an indicator for formation of autophagosomes, its cellular levels are difficult to interpret. For example, different patterns can indicate autophagy activation:

LC3-I decreases and LC3-II increases due to rapid conversion of LC3-I to LC3-II.

LC3-II decreases in comparison to LC3-I, because LC3-II is degraded in lysosomes, too, if the autophagy process proceeds.
LC3-I and LC3-II both decrease due to rapid conversion of LC3-I to LC3-II and rapid degradation of LC3-II [49].
To tackle this problem, the use of BafilomycinA1 (a macrolid antibiotic) interrupts the autophagic pathway and thereby is helpful to differentiate the causes of high LC3-II measurements. If high LC3-II levels are the result of increased autophagosome formation, LC3-II levels will further increase under Bafilomycin A1 treatment, because it inhibits the LC3-II degradation. If the enhancement is due to decreased degradation of autophagolysosomes, treatment with BafilomycinA1 will not alter LC3-II levels. This protocol could be applied when investigating cells in cell culture and incubate them with the antibiotic for several hours prior to western blotting [59, 60]. Unfortunately, one still can not rely on LC3 only as an indicator for autophagosome formation and autophagic structure, even if properly detected. This was exemplified by an experiment in animal model with homozygous deletion of Beclin1 (aiming for interruption of autophagosome formation), showing that LC3-II was still formed even though autophagosome formation was interrupted. In contrast, when Atg5 was deleted (also aiming for interruption of autophagosome formation), no LC3-II was formed then. Additionally, LC3-II may also colocalize with non-autophagic structures („ectopically“) [49].

To state that the found increase in LC3B-II levels in this experiment was due to increased LC3B-I synthesis and conversion through high autophagy activity remains unclear. Also, even though high LC3B-II levels might represent autophagosome formation, there is no say that the whole autophagic degradation process was intact and upregulated. Interestingly, Li, Y. et al. (2021) showed elevated levels of LC3-II in Dahl salt-sensitive rats, regardless that some of them did not develop hypertension. Among the HSD fed rats, they divided subgroups of rats which developed manifest hypertension (<150 mmHg systolic blood pressure), hypertension susceptibility (130-150 mmHg) and some remained hypertension-resistent (<130 mmHg). All of those had significantly higher LC3-II levels compared to a low-salt fed control group. In synopsis with their results, they stated that HSD has blood-pressure independent deteriorating effects not only on the heart, but on other organs too. Regarding heart function, they concluded that high salt overly

activates autophagy and leads to weak heart function [61].

This is in some contrast to the findings of Eisenberg, T. et al. (2016). They investigated the effect of spermidine on life-span extension in different rodent models. First, they were able to show that wild-type C57BL/6J mice, a wide-spread mouse model also for research on aging, supplied with spermidine had prolonged life-span in comparison to the group without spermidine intake. Also, the spermidine-fed mice showed better cardiac performance in comparison to their spermidine-abstinent contemporaries (e.g. better diastolic function and reduction in left ventricular hypertrophy). Further, they had enhanced autophagy (measured *in-vivo* autophagic flux, leupeptid assay, LC3-II was increased) and mitophagy (using Mito-Keima mice, under spermidine treatment increased Mito-Keima positive area indicating mitophagy). In Dahl salt-sensitive rats, which developed hypertension-induced HFpEF on HSD, they could show that the group additionally fed on spermidine showed slower progression of hypertension, had more preserved diastolic function and lower heart weight than the group which did not receive spermidine. They did not measure autophagy-related proteins in heart tissue, but out of renal tissue (renal pathologies in Dahl salt-sensitive rats go along with hypertension induction), and found that p62 is decreased in spermidin-treated rat kidneys, suggesting autophagy induction. To substantiate the assumption that the benefitial cardiovascular effect mechanism of spermidin involves autophagy, they used mice with homozygous cardiomyocyte-specific deletion of the Atg5 gene (Atg5-/-) to abolish autophagy. This ultimately resulted in total lack of LC3-II and increased p62 levels in the cardiomyocytes, and adverse cardiac remodelling is preprogrammed. Despite the spermidine administration, a reduction of cardiac remodelling was not observed like in the Atg5 positive control group, indicating that spermidine has autophagy-dependent beneficial effects. So autophagy induction in Dahl salt-sensitive rats was competent to rescue the hypertension-induced phenotype to some degree, also leading to the assumption that low autophagy activity was partly causing poor heart function [62].

Regarding the question whether the elevated LC3B-II levels in our Dahl rats represented high or low autophagy activity, these ambiguous findings of Eisenberg, T. et al. (2016) and Li Y et al (2021) and the limitation of the detection method do not allow a clear decision with our data. The non-consistent finding in the LC3B ratio could be due to the distortion of the ratio because of different antibody affinity, to

some degree. Also adding the difficulties by quantification of both forms in this experiment. While LC3B-II presented with a clear distinguishable band, LC3B-I was far more cloudy and harder to define. Therefore, for the future I would recommend performing an assay capable of assessing autophagosome turnover, parallelly to LC3-II detection, to determine if an elevated LC3-II level is consistent with an actual increase in autophagic degradation, anyway. Also, a comprehensive sample size could help to clear the results for p62, if there is an apparent increase in this protein, it would indicate low autophagic activity.

Mice with cardiomyocyte specific deletion of Atg5 develop left ventricular hypertrophy, finally causing heart failure and mitochondrial dysfunction. It is discussed that other Atg5 independent autophagy mechanism could be upregulated for compensation, but this only seems to work temporarily or inefficient, since mice develop heart failure, nonetheless. Ljubojević-Holzer, S. et al. (2021) verified both decreased Atg5 gene and protein expression in human hypertrophied and failing left ventricular myocardium, alongside a decrease of other autophagy markers [19, 51]. Other findings also confirm, that levels of Atg5 should be decreased in aged myocardium, indicating an impaired autophagy mechanism [48]. Here, we could not detect a significant change in Atg5 levels between LSD and late timepoint of HSD. If there is no major change detected in the amount of Atg5, fluorescence assay could uncover underlying autophagic activity. In cells with low autophagic activity, Atg5 fluorescence is distributed diffusely in the cytoplasm, while in autophagy induction a punctate pattern develops [49].

Takakura, K. et al. (2017) studied the effect of cordycepin in hypertensive Dahl salt-sensitive rats. Cordycepin is an analogue of adenosine, which highly accumulates in the sac fungus *Cordaceps militaris*. At an age of 5 weeks, they started the rats on different diets. The group serving as control received HSD only and the cordycepin group received HSD and cordycepin. Both groups developed hypertension, but there was a difference in the expression of autophagy markers. In heart, kidneys and liver they found, that in the cordycepin group the LC3 ratio was enhanced, p62 and mTOR ratio were decreased in comparison with the control group. They inferred that autophagy was upregulated under cordycepin treatment. Moreover, cordycepin treated rats had prolonged lifespan and light- and electron-microscopy revealed better cardiomyocyte condition since mitochondria were superior in score and

structure. The decrease in the mTOR ratio means, that the share of the activated, phosphorylated mTOR form was lower in the cordycepin rats, indicating that mTOR signaling in hypertensive Dahl salt-sensitive rats is higher than in individuals with autophagy induction due to cordycepin [63]. Since cardiomyocytes could be considered healthier in cordycepin treatment (with upregulated autophagy and mitophagy), autophagy downregulation in hypertensive Dahl salt-sensitive rats could be contributing to the worsening cardiac function. Still, in our experiment, no alteration in the mTOR ratio was found between the control group and early and late stage of cardiac remodelling. But even no significant finding was made, it seems like in the late stage of cardiac remodelling, mTOR is tending to elevation. Indeed, there is almost no change in the activated, phosphorylated form, but this development might be worthy to look into detail in further investigation.

Xiong, W. et al. (2018) found that in mitophagy mito-Parkin levels increased alongside with Pink1 levels, consistent with the Pink1 dependent mechanism of Parkin direction to mitochondria [52]. In this thesis experiment, there was no quantification of mito-Parkin, rather total Parkin levels out of whole cell lysate were detected. But since there was no change in Pink1 levels, it is questionable if the impressive increase in Parkin in late HSD group is due to increased levels of mito-Parkin, since there is no expressiveness about the amount of Parkin bound to mitochondria. In this experiment, it remained unclear, if there was also an increased translocation of Parkin to mitochondria as a result of upregulated mitophagy. For isolated detection of mito-Parkin, cell fractionating and investigation of the mitochondria-rich fraction would also be an option for the future. The allegation, that western blotting is too insensitive for the detection of Pink1 amounts, is not supported by the fact that other authors showed strong Pink1 expressions ([64] in HeLa Cells). And since the detected bands of Pink1 in mice were very weak and did not match the manufacturer ‘s depiction, I rather suspect that the detection of Pink1 was not optimal and needs adaption.

4.3 Autophahy in human diastolic dysfunction

As a hallmark of heart failure, NCX1 and SERCA2a showed no significant change, however patients did not yet present with heart failure but diastolic dysfunction. But like before mentioned, a trend to elevated NCX1 levels can be assumed and fits the idea of beginning cardiac remodelling and dysfunction.

The results concerning autophagy can be pre-summarized with no significant change and no striking trend of any investigated protein apart from Pink1, which shows a trend to decreased levels.

Hahn, V. S. et al. (2021), performed RNA sequencing on right ventricular human myocardium from HFpEF patients, so these hearts had already proceeded from diastolic dysfunction to heart failure. They investigated HFpEF specific alteration in gene expression and concluded that in HFpEF autophagy-related genes were down-regulated [40]. The finding of altered autophagic activity could not be confirmed in this experiment, since results of p62, Atg5 and LC3B-II did not indicate any sturdy changes. Notewothy is, that our samples were from non-failing hearts and the detection method ‚western blotting' is less sensitive than RNA analysis. Even though Hahn, V. S. et al. (2021) results could not be confirmed, our experiment did not show contradictory results. For further investigations I would recommend detecting autophagy markers in manifest HFpEF, additionally to samples from diastolic dysfunction.

When assuming that autophagy should be downregulated in diastolic dysfunction, mTOR and p-mTOR would be expected to increase and/or the mTOR ratio should be increased. In our conducted experiment, we could not confirm such a development, again holding in mind, that our samples originated from patients with diastolic dysfunction only. As recommended, it would be interesting to further investigate the markers in manifest HFpEF in humans.

A study of Chen, X. et al. (2022) dealt, among others, with mitochondrial function in HFpEF. They made use of C57BL/6J mice, some of them were wilde-type, some telomerase deficient. In all animals, they induced HFpEF with high fat diet and L-NAME (Nω-Nitro-L-arginine methyl ester hydrochloride). Control animals received chow diet. HFpEF proceeded faster in telomerase knockout mice. Immunoblotting was competent to detect elevated levels of p53 in cardiomyocytes, which is thought

to disrupt mitochondrial function, mitophagy and therefore cardiac function. Consistent with this, they showed that HFpEF was alleviated in myocyte-specific p53 knockout mice, when HFpEF was dietary induced [65, 66]. If we assume low mitophagic activity in HFpEF, we could also think of lower levels of Parkin and Pink1 in diastolic dysfunction. Here, we found no significant change in both kinases, although few samples had decreased Pink1 levels. Investigation of the mitochondria-rich cell fraction could deliver further details about mitophagy activity (*like in the previous chapter, 4.2*). Also, an increased sample size could be able to show an apparent difference in Pink1 levels between the control and diastolic dysfunction group.

4.4 Autophagy in human dilated cardiomyopathy (DCM)

As a hallmark of heart failure, NCX1 was significantly increased in DCM patients, whereas SERCA2a levels were not decreased, although expected. Caragnano, A. et al. (2019) investigated autophagy markers in human cardiac samples with DCM. An important finding was that autophagy was disrupted, with accumulation of p62, increased mTOR activation and dysfunctional mitochondria accompanied by increased Parkin levels, probably as a surrogate for stimulated mitophagy [15]. Except for mTOR, these effects could not be reproduced in this thesis, irrefutably. The five patients showed no striking change of p62, Atg5 or LC3B-II. But levels of p-mTOR and mTOR were significantly increased, coping with the finding that mTOR signaling in DCM patients is increased and indicating disruption of autophagy.

This is in contrast to the results obtained by Jin, B. et al. (2020), who induced and inhibited autophagy in DCM mouse model and studied the effect on autphagy activity and heart function. Levels of p-mTOR and LC3II were assessed by western blotting. The group with DCM, which was administered the autophagy-inducer rapamycin (mTOR inhibitor) showed elevated levels of LC3-II and decreased levels of p-mTOR, as a surrogate for activated autophagy. Furthermore, their cardiac performance was better than in the DCM only group. Vice versa, the DCM group administered with the autophagy-inhibitor 3-MA (3-methyadenine) showed the contrary effect. There were decreased levels of LC3-II and increased levels of p-mTOR, as a surrogate for repressed autophagy and cardiac performance was worse than in DCM only mice. In this model, the DCM only group showed lower p-mTOR and higher LC3-II levels compared to control, indicating that autophagy is upregulated in the disease [67]. This is probably a compensatory mechanism and is not consistent with the finding in human DCM hearts, where autophagy seems to be disrupted. Since autophagy induction had beneficial effects onto the course of the disease in the mouse model, I suggest the possibility, that the compensatory upregulation of autophagy in the human hearts was exhausted or failed to establish in the first place.

As before mentioned, the increased Parkin levels found by Caragnano, A. et al. (2019) were not confirmed in our experiment. On the contrary, Pink1 levels trended to lower levels, which cannot be explained to some extent, as it would indicate supressed mitophagy, if this was a real development.

4.5 Comparison of Dahl salt-sensitive rats with human diastolic dysfunction

Admittedly, there are incongruities in the opinon on autophagy in HFpEF (and diastolic dysfunction). Yang, H.-J. et al. (2020) showed that in diet-induced HFpEF mice, autophagy was induced, which goes along with the autophagy induction in hypertensive Dahl salt-sensitive rats, which develop HFpEF, too [68]. This seems to be in contrast with the findings of Hahn, V. S. et al. (2021), where autophagy was downregulated in human hearts with HFpEF [40]. Even though that this is a comparison of humans with two different model species, it is inconvenient to see oppositional effects.

The early timepoint HSD group of the Dahl salt-sensitive rat was expected to represent diastolic dysfunction and is therefore compared to the human samples acquired from diastolic dysfunction patients.

In both rats and humans, a striking decrease of SERCA2a failes to appear, but NCX1 shows uprising trends for both, even though they are not significant in that stage of disease. More similarities are shared in the finding, that p62, Atg5, LC3B-II, LC3B ratio, Parkin and mTOR proteins hold off significant changes. For LC3B-II and Parkin in the rat samples, a significant increase was reached after progress to the late timepoint on HSD (representing late stage of cardiac remodelling, aiming for HFpEF). If this development is similar in humans, samples from apparent HFpEF patients need to be investigated as well.

To note, when comparing LC3 levels of different cell types, it must be regarded that levels and ratios differ. Also, isoforms of LC3 (LC3A, LC3B and LC3C) differ depending on cell type. This also applies for comparison of different species (e.g. human and rat) [49].

Interestingly, in humans Pink1 is trending to lower levels compared to control, while in rats Pink1 shows no great change. The used antibody for Pink1 detection was designed for rat, mouse and human tissue. But a checkout of the antibody revealed, that Pink1 detection in mice was working good, while in humans and rats the bands revealed as comparatively very weak. Therefore, making suggestions on mitophagy would be to vague and speculative. Rather adaption of the detection of mitophagy parameters should be pursued (differentiate mito-and cyto-Parkin, re-evaluate antibodies).

5 Conclusion

First of all, despite the frequent lack of significant findings in this setting, this does not mean that there is no effect. Given the small sample number, a non-significant trend or even no observed effect at all could become significant or overt in an experiment with adequate sample number. The other way around, a highly significant effect observed in this setting could be accidental by chance and might balance out in an experiment with adequate sample number.

With regard to other data and experiments, we rather expected autophagy downregulation in hypertensive Dahl salt-sensitive rats. The ambigous finding of elevated LC3-II levels and supposedly uptrending p62 are in contrast to each other and additional assays would help to clarify especially the meaning of the LC3-II increase. To facilitate the interpretation of the other autophagy markers, we need to increase the sample size in further experiments to look for significant effects.

Our findings in human diastolic dysfunction showed no change at all and there is little literature about autophagy in diastolic dysfunction to compare to. In manifest HFpEF we would expect downregulated autophagy from other human data and downregulated mitophagy from mice experiments. To reproduce these findings in HFpEF, diastolic dysfunction seemed not to be sufficient enough and no such change in autophagic activity could be detected.

In human DCM, the elevation in p-mTOR and mTOR could confirm findings from another study with human samples, indicating that autophagy is disrupted. Yet, other autophagy markers in our experiment failed to confirm this finding. Also, we could not show induction of mitophagy with our parameters.

In summary, for further perspectives I would suggest enhancing the sample size and complement the current detection method with additional assays in order to assess the autophagic flux. This would help to classify simply elevated or decreased levels in immunoblotting as autophagy induction or inhibition.

6 Bibliography

1. Yang, Z. and D.J. Klionsky, *Eaten alive: a history of macroautophagy.* Nat Cell Biol, 2010. **12**(9): p. 814-22.
2. Mizushima, N. and M. Komatsu, *Autophagy: renovation of cells and tissues.* Cell, 2011. **147**(4): p. 728-41.
3. Tooze, S.A. and T. Yoshimori, *The origin of the autophagosomal membrane.* Nat Cell Biol, 2010. **12**(9): p. 831-5.
4. Zachari, M. and I.G. Ganley, *The mammalian ULK1 complex and autophagy initiation.* Essays Biochem, 2017. **61**(6): p. 585-596.
5. Zhang, M., et al., *Correction: SOCS5 inhibition induces autophagy to impair metastasis in hepatocellular carcinoma cells via the PI3K/Akt/mTOR pathway.* Cell Death Dis, 2019. **10**(11): p. 799.
6. Randall-Demllo, S., M. Chieppa, and R. Eri, *Intestinal epithelium and autophagy: partners in gut homeostasis.* Front Immunol, 2013. **4**: p. 301.
7. Katsuragi, Y., Y. Ichimura, and M. Komatsu, *p62/SQSTM1 functions as a signaling hub and an autophagy adaptor.* Febs j, 2015. **282**(24): p. 4672-8.
8. Nakamura, S. and T. Yoshimori, *New insights into autophagosome-lysosome fusion.* J Cell Sci, 2017. **130**(7): p. 1209-1216.
9. Abdellatif, M., et al., *Autophagy in Cardiovascular Aging.* Circ Res, 2018. **123**(7): p. 803-824.
10. Szwed, A., E. Kim, and E. Jacinto, *Regulation and metabolic functions of mTORC1 and mTORC2.* Physiol Rev, 2021. **101**(3): p. 1371-1426.
11. Tan, V.P. and S. Miyamoto, *Nutrient-sensing mTORC1: Integration of metabolic and autophagic signals.* J Mol Cell Cardiol, 2016. **95**: p. 31-41.
12. Sardiello, M., *Transcription factor EB: from master coordinator of lysosomal pathways to candidate therapeutic target in degenerative storage diseases.* Ann N Y Acad Sci, 2016. **1371**(1): p. 3-14.
13. Sciarretta, S., et al., *The Role of Autophagy in the Heart.* Annu Rev Physiol, 2018. **80**: p. 1-26.
14. Schaefer, L., *Complexity of danger: the diverse nature of damage-associated molecular patterns.* J Biol Chem, 2014. **289**(51): p. 35237-45.
15. Caragnano, A., et al., *Autophagy and Inflammasome Activation in Dilated Cardiomyopathy.* J Clin Med, 2019. **8**(10).

16. Kaushik, S. and A.M. Cuervo, *Chaperones in autophagy.* Pharmacol Res, 2012. **66**(6): p. 484-93.
17. Jackson, M.P. and E.W. Hewitt, *Cellular proteostasis: degradation of misfolded proteins by lysosomes.* Essays Biochem, 2016. **60**(2): p. 173-180.
18. Kaushik, S. and A.M. Cuervo, *The coming of age of chaperone-mediated autophagy.* Nat Rev Mol Cell Biol, 2018. **19**(6): p. 365-381.
19. Abdellatif, M., et al., *Autophagy in cardiovascular health and disease.* Prog Mol Biol Transl Sci, 2020. **172**: p. 87-106.
20. Fidziańska, A., E. Walczak, and M. Walski, *Abnormal chaperone-mediated autophagy (CMA) in cardiomyocytes of a boy with Danon disease.* Folia Neuropathol, 2007. **45**(3): p. 133-9.
21. Damme, M., et al., *Autophagy in neuronal cells: general principles and physiological and pathological functions.* Acta Neuropathol, 2015. **129**(3): p. 337-62.
22. Tan, H.W.S., A.Y.L. Sim, and Y.C. Long, *Glutamine metabolism regulates autophagy-dependent mTORC1 reactivation during amino acid starvation.* Nat Commun, 2017. **8**(1): p. 338.
23. Yang, Z. and D.J. Klionsky, *Permeases recycle amino acids resulting from autophagy.* Autophagy, 2007. **3**(2): p. 149-50.
24. Nah, J., D. Zablocki, and J. Sadoshima, *Autosis: A New Target to Prevent Cell Death.* JACC Basic Transl Sci, 2020. **5**(8): p. 857-869.
25. Liu, Y., et al., *Autosis is a Na+,K+-ATPase-regulated form of cell death triggered by autophagy-inducing peptides, starvation, and hypoxia-ischemia.* Proc Natl Acad Sci U S A, 2013. **110**(51): p. 20364-71.
26. Lavandero, S., et al., *Autophagy in cardiovascular biology.* J Clin Invest, 2015. **125**(1): p. 55-64.
27. Zhu, H., et al., *Cardiac autophagy is a maladaptive response to hemodynamic stress.* J Clin Invest, 2007. **117**(7): p. 1782-93.
28. Vandenabeele, P., et al., *Molecular mechanisms of necroptosis: an ordered cellular explosion.* Nat Rev Mol Cell Biol, 2010. **11**(10): p. 700-14.
29. Kobayashi, S., et al., *Transcription factor GATA4 inhibits doxorubicin-induced autophagy and cardiomyocyte death.* J Biol Chem, 2010. **285**(1): p. 793-804.

30. Kim, I., S. Rodriguez-Enriquez, and J.J. Lemasters, *Selective degradation of mitochondria by mitophagy.* Arch Biochem Biophys, 2007. **462**(2): p. 245-53.
31. Lemasters, J.J., *Variants of mitochondrial autophagy: Types 1 and 2 mitophagy and micromitophagy (Type 3).* Redox Biol, 2014. **2**: p. 749-54.
32. Dorn, G.W., 2nd, *Parkin-dependent mitophagy in the heart.* J Mol Cell Cardiol, 2016. **95**: p. 42-9.
33. Narendra, D., et al., *Parkin is recruited selectively to impaired mitochondria and promotes their autophagy.* J Cell Biol, 2008. **183**(5): p. 795-803.
34. Lin, Y.F. and C.M. Haynes, *Metabolism and the UPR(mt).* Mol Cell, 2016. **61**(5): p. 677-682.
35. McDonagh, T.A., et al., *2021 ESC Guidelines for the diagnosis and treatment of acute and chronic heart failure.* Eur Heart J, 2021. **42**(36): p. 3599-3726.
36. Gregory Gibson, M.V.B., MD; Robert John Mentz, MD, FACC; Anuradha (Anu) Lala, MD, FACC, *Universal Definition and Classification of Heart Failure: A Step in the Right Direction from Failure to Function.* American College of Cardiology 2021.
37. Pfeffer, M.A., A.M. Shah, and B.A. Borlaug, *Heart Failure With Preserved Ejection Fraction In Perspective.* Circ Res, 2019. **124**(11): p. 1598-1617.
38. Loffredo, F.S., et al., *Heart failure with preserved ejection fraction: molecular pathways of the aging myocardium.* Circ Res, 2014. **115**(1): p. 97-107.
39. Hamdani, N., et al., *Myocardial titin hypophosphorylation importantly contributes to heart failure with preserved ejection fraction in a rat metabolic risk model.* Circ Heart Fail, 2013. **6**(6): p. 1239-49.
40. Hahn, V.S., et al., *Myocardial Gene Expression Signatures in Human Heart Failure With Preserved Ejection Fraction.* Circulation, 2021. **143**(2): p. 120-134.
41. Bozkurt, B., et al., *Current Diagnostic and Treatment Strategies for Specific Dilated Cardiomyopathies: A Scientific Statement From the American Heart Association.* Circulation, 2016. **134**(23): p. e579-e646.
42. Tayal, U., et al., *Understanding the genetics of adult-onset dilated cardiomyopathy: what a clinician needs to know.* European Heart Journal, 2021. **42**(24): p. 2384-2396.
43. McNally, E.M. and L. Mestroni, *Dilated Cardiomyopathy: Genetic Determinants and Mechanisms.* Circ Res, 2017. **121**(7): p. 731-748.

44. Johnston, J.A., C.L. Ward, and R.R. Kopito, *Aggresomes: a cellular response to misfolded proteins.* J Cell Biol, 1998. **143**(7): p. 1883-98.
45. Gianni, D., et al., *Protein aggregates and novel presenilin gene variants in idiopathic dilated cardiomyopathy.* Circulation, 2010. **121**(10): p. 1216-26.
46. Aleksova, A., et al., *Interleukin-1β levels predict long-term mortality and need for heart transplantation in ambulatory patients affected by idiopathic dilated cardiomyopathy.* Oncotarget, 2017. **8**(15): p. 25131-25140.
47. Studer, R., et al., *Gene expression of the cardiac Na(+)-Ca2+ exchanger in end-stage human heart failure.* Circ Res, 1994. **75**(3): p. 443-53.
48. Hua, Y., et al., *Chronic Akt activation accentuates aging-induced cardiac hypertrophy and myocardial contractile dysfunction: role of autophagy.* Basic Res Cardiol, 2011. **106**(6): p. 1173-91.
49. Klionsky, D.J., et al., *Guidelines for the use and interpretation of assays for monitoring autophagy (4th edition)(1).* Autophagy, 2021. **17**(1): p. 1-382.
50. Jiang, P. and N. Mizushima, *LC3- and p62-based biochemical methods for the analysis of autophagy progression in mammalian cells.* Methods, 2015. **75**: p. 13-8.
51. Ljubojević-Holzer, S., et al., *Loss of autophagy protein ATG5 impairs cardiac capacity in mice and humans through diminishing mitochondrial abundance and disrupting Ca2+ cycling.* Cardiovasc Res, 2022. **118**(6): p. 1492-1505.
52. Xiong, W., et al., *PTEN induced putative kinase 1 (PINK1) alleviates angiotensin II-induced cardiac injury by ameliorating mitochondrial dysfunction.* Int J Cardiol, 2018. **266**: p. 198-205.
53. Kim, Y.C. and K.L. Guan, *mTOR: a pharmacologic target for autophagy regulation.* J Clin Invest, 2015. **125**(1): p. 25-32.
54. Dunlay, S.M., V.L. Roger, and M.M. Redfield, *Epidemiology of heart failure with preserved ejection fraction.* Nat Rev Cardiol, 2017. **14**(10): p. 591-602.
55. Inoko, M., et al., *Transition from compensatory hypertrophy to dilated, failing left ventricles in Dahl salt-sensitive rats.* Am J Physiol, 1994. **267**(6 Pt 2): p. H2471-82.
56. Gallet, R., et al., *Cardiosphere-derived cells reverse heart failure with preserved ejection fraction (HFpEF) in rats by decreasing fibrosis and inflammation.* JACC Basic Transl Sci, 2016. **1**(1-2): p. 14-28.

57. Zhang, W., et al., *Morphometric, Hemodynamic, and Multi-Omics Analyses in Heart Failure Rats with Preserved Ejection Fraction.* Int J Mol Sci, 2020. **21**(9).
58. Gottlieb, R.A., et al., *Untangling autophagy measurements: all fluxed up.* Circ Res, 2015. **116**(3): p. 504-14.
59. Loos, B., A. du Toit, and J.H. Hofmeyr, *Defining and measuring autophagosome flux—concept and reality.* Autophagy, 2014. **10**(11): p. 2087-96.
60. Mauvezin, C. and T.P. Neufeld, *Bafilomycin A1 disrupts autophagic flux by inhibiting both V-ATPase-dependent acidification and Ca-P60A/SERCA-dependent autophagosome-lysosome fusion.* Autophagy, 2015. **11**(8): p. 1437-8.
61. Li, Y., et al., *Nitric Oxide Alleviated High Salt-Induced Cardiomyocyte Apoptosis and Autophagy Independent of Blood Pressure in Rats.* Front Cell Dev Biol, 2021. **9**: p. 646575.
62. Eisenberg, T., et al., *Cardioprotection and lifespan extension by the natural polyamine spermidine.* Nat Med, 2016. **22**(12): p. 1428-1438.
63. Takakura, K., et al., *Cordyceps militaris improves the survival of Dahl salt-sensitive hypertensive rats possibly via influences of mitochondria and autophagy functions.* Heliyon, 2017. **3**(11): p. e00462.
64. Sato, S. and N. Furuya, *Induction of PINK1/Parkin-Mediated Mitophagy.* Methods Mol Biol, 2018. **1759**: p. 9-17.
65. Chen, X., et al., *p53-Dependent Mitochondrial Compensation in Heart Failure With Preserved Ejection Fraction.* J Am Heart Assoc, 2022. **11**(11): p. e024582.
66. Del Campo, A., et al., *Mitochondrial function, dynamics and quality control in the pathophysiology of HFpEF.* Biochim Biophys Acta Mol Basis Dis, 2021. **1867**(10): p. 166208.
67. Jin, B., et al., *Up-regulating autophagy by targeting the mTOR-4EBP1 pathway: a possible mechanism for improving cardiac function in mice with experimental dilated cardiomyopathy.* BMC Cardiovasc Disord, 2020. **20**(1): p. 56.

68. Yang, H.J., et al., *MD1 deletion exaggerates cardiomyocyte autophagy induced by heart failure with preserved ejection fraction through ROS/MAPK signalling pathway.* J Cell Mol Med, 2020. **24**(16): p. 9300-9312.

7 Supplements

7.1 *In vivo* data of whole cohort

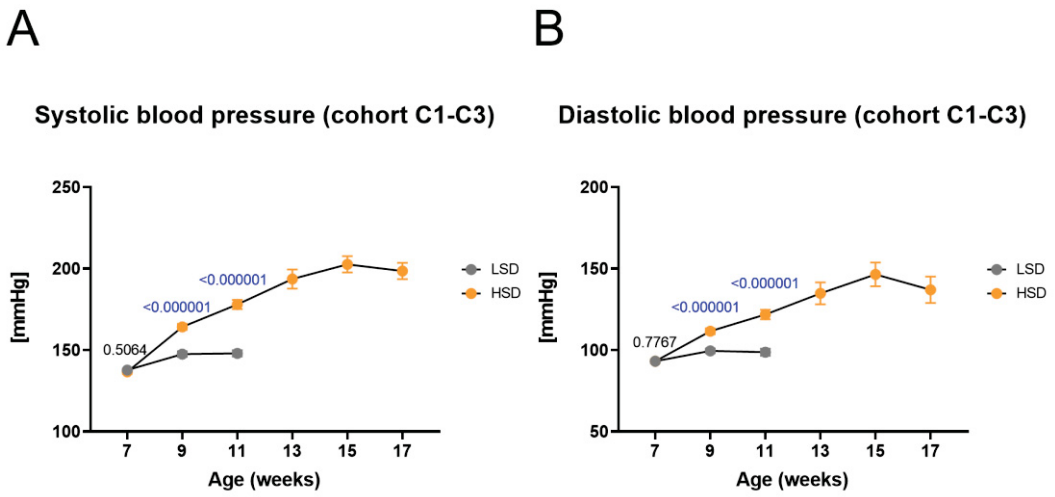

Figure 7-1: Blood pressure measurements of Dahl salt-sensitive rats of whole cohort. Changes in systolic [A] and diastolic [B] blood pressure in Dahl salt-sensitive rats on respective diets. LSD and HSD (early timepoint until week 12, late timepoint until week 17). P<0.05 was considered significant. By courtesy of Holzer, Senka PhD and Voglhuber, Julia MSc.

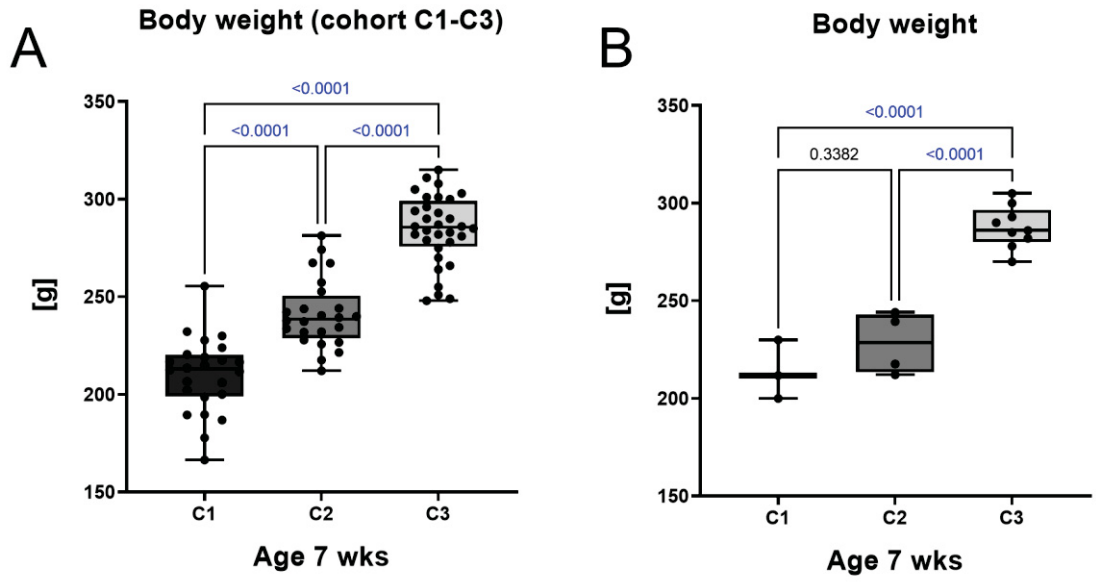

Figure 7-2: Body weight in gram [g] **of Dahl salt-sensitive rats at age of 7 weeks** prior to special treatment. [A] Body weight of all rats utilized by the working group Holzer and [B] body weight of all rats investigated for this thesis. P<0.05 was considered significant. By courtesy of Holzer, Senka PhD and Voglhuber, Julia MSc.